A Thesis for the Degree of Master of Engineering

Stability Analysis of Unsaturated Sand Slope Considering Suction Stress Concept

Advisor Kim, Tae-Hyung

December, 2010

Graduated School of Korea Maritime University

Department of Civil and Environmental Engineering
Lee, Nam Woo

工學碩士 學位論文

흡입응력 개념을 적용한 불포화 모래사면의 안정 해석

Stability Analysis of Unsaturated Sand Slope Considering Suction Stress Concept

指導敎授　金 泰 亨

2010年　12月

韓國海洋大學校 大學院

土木環境工學科

李 南 雨

本 論文을 李南雨의 工學碩士 學位論文으로 認准함.

委員長　　宋　泳　錫　　(印)

委　員　　徐　榮　敎　　(印)

委　員　　金　泰　亨　　(印)

2010年　12月

韓國海洋大學校 大學院

CONTENTS

List of Tables

List of Figures

Stability Analysis of Unsaturated Sand Slope Considering Suction Stress Concept

by
Lee, Nam Woo

Department of Civil and Environmental Engineering
Graduate School of
Korea Maritime University

Abstract

In this study, a stability analysis of unsaturated sand slope existing water table is conducted considering suction stress concept. It is assumed that slope is composed of sand with the range of relative densities 40%, 60%, and 75%, respectively. The analysis considers the ground water level located at depth of 5m below the ground surface, and variation of suction stress, moisture content and matric suction above the water table under steady infiltration rate conditions. To analyze the stability of unsaturated sand slope, the Soil Water Characteristics Curve (SWCC) of the sand with the range of relative densities 40%, 60%, and 75% were measured using the automated SWCC apparatus. Based on the SWCC, the Suction Stress

Characteristics Curve (SSCC) and the Hydraulic Conductivity Function (HCF) were estimated by van Genuchten (1980)'s SWCC fitting parameters both drying and wetting processes. The stability analysis of unsaturated sand slopes was carried out under no infiltration and steady infiltration rate conditions using these experimental results.

As the results of stability analysis, under no infiltration condition, the factor of safety is increased at the zone between 0 to 0.4m above the water table due to effect of suction stress. However, under infiltration rate conditions, the factor of safety is increased at the all depths in slope due to effect of suction stress. Of course, as infiltration rate approaches the value of the saturated hydraulic conductivity, the stability of sand slopes are decreased due to decreasing suction stress. However, slopes are maintained in a more stable states under steady infiltration rate conditions than no infiltration condition. It is confirmed that the unsaturated sand is reached to pendular state at the relatively small matric suction range, and suction stress does not occurred at all depths in slope under no infiltration.

흡입응력 개념을 적용한 불포화 모래사면의 안정 해석

이 남 우

토목환경공학과
한국해양대학교 대학원

요 지

본 연구에서는 지하수위가 존재하는 불포화 무한사면의 안정해석을 흡입응력 개념을 이용하여 수행하였다. 이를 위해 상대밀도 40%, 60%, 75%로의 사질토로 이루어진 사면을 가정하였다. 이 해석에서는 지표면으로부터 5m 아래 지하수위를 고려하였으며, 정상침투시 지하수위 이상의 깊이에서 흡입응력 및 체적함수비, 모관흡수력의 변화도 고려하였다. 불포화 모래사면의 안정 해석을 실시하기 위해 자동 흙-함수특선곡선 측정장치를 활용하여 상대밀도 40%, 60%, 75%의 모래에 대한 흙-함수특성곡선(Soil Water Characteristic Curve, SWCCs)을 산정하였다. 또한 van Genuchten 경험식에 의한 흙-함수특성곡선 계수를 이용하여 건조 및 습윤과정에 따른 흡입응력특성곡선(Suction Stress Characteristics Curve, SSCC)과 투수계수함수(Hydraulic Conductivity Function, HCF)을 산정하였다. 이러한 시험적 불포화토의 고유 물성치를 이용하여 비침투 및 정상침투시 불포화 모래사면에 대한 안정해석이 이루어졌다.

그 결과, 강우침투가 없는 조건에서는 흡입응력이 미치는 지하수위로부터 0~0.4m 높이까지 안전율에 증가를 보이지만, 강우침투시 사면 전 깊이에서 발

생되는 흡입응력의 영향으로 인해 사면 전 깊이에서 안전율의 증가하는 경향을 보였다. 물론 침투율이 포화투수계수와 가까워짐에 따라 사면의 안전율 증가량이 감소하는 경향을 보이고 있지만 침투가 없는 조건에 비해 사면이 보다 안정한 상태로 유지된다. 이러한 결과는 비교적 작은 모관흡수력 범위에서 모래의 상태가 pendular 영역에 도달한 점과 이로 인해 흡입응력이 사면 전 깊이에 걸쳐 발생되지 않는 점에 기인된 결과로 사료된다.

Chapter 1. Introduction

1.1 Necessity and objective

Rainfall is the most important factor occurring landslide, because most of the landslides are occurred during the rainy season. In Korea, most of annual rainfall is concentrated on from June to September. During this period, the occurrence of landslides due to torrential rains are frequent and growing each year resulting in landslides (Hong et al., 1990; Park et al., 2008). Most of the landslides occurred in Korea are appeared in the form of a shallow plane failure within 2m in depth (Hong and Song, 2006; Kim et al., 2007). Because of the infiltration of rainfall, degree of saturation of unsaturate ground located at high level of ground-water levels is increased and matric suction is decreased.

Unsaturated soil is conceptualized as partially saturated soil which is intermediate range between dry soil and saturated soil. It has different behavior characteristic compared to saturated soil. Therefore, it is important to estimate the soil parameters for unsaturated soil, such as Soil Water Characteristic Curve (SWCC), Hydraulic Conductivity Function (HCF), and Suction Stress Characteristic Curve (SSCC) related with strength of unsaturated soil. Many researchers have been conducted on estimating the ground parameters and analyzing the behavior for unsaturated soil is mainly conducted (Jennings and Burland, 1962; Fredlund and Morgenstern, 1977; Fredlund et al., 1978; Lu and Likos, 2006; Lu et al., 2007, 2009; Chae et al., 2010; Kim and Kim, 2010).

The stability of natural and engineered earthen slope is a classical subject in soil mechanics, slope hydrology, and geomorphology (Lu and Godt, 2008). In Korea, until recently, most slope stability analysis has been based on Terzaghi's effective stress principle in which pore water pressure is quantified by saturated seepage theories (Cho, 2000). However, in well-drained colluvial soils, shallow slope failures may occur within the vadose zone under partially saturated soil conditions (Wolle and Hachich, 1989; de Campos et al., 1991; Godt et al., 2006). When the moisture variation in the vertical direction in hillslope is important, the consequent effective stress above the water table may need to be considered rigorously. The effective stress in partially saturated soil is no longer the difference between the total stress and pore-water pressure or soil suction. The generalized effective stress which unifies both saturated and unsaturated conditions has been proposed by Lu and Likos (2004, 2006) considering suction stress, which is conceptualized as the resultant of interparticle physicochemical stresses.

Therefore, the aim of in this study is to analyze how generalized effective stress or suction stress can be affected to stability of infinite slope under unsaturated condition.

1.2 Thesis organization

The thesis is divided into five chapters.

Chapter 2 introduces background of unsaturated soil mechanics, such as matric suction, general Soil Water Characteristic Curve (SWCC), and major cause of hysteresis between drying SWCC and wetting SWCC.

Chaper 3 introduces overall composition and principle of Automated SWCC Experiments as well as shows the characteristic of soil sample using in this study.

Chapter 4 shows the Experimental results and analysis. As the results, matric suction and volumetric water content for three sands within the range of relative densities 40%, 60%, and 75% are measured using automated SWCC apparatus both drying and wetting. Using this experimental results, SWCC and Hydraulic Conductivity Function (HCF) is estimated by van Genuchten (1980)'s model. Moreover, Suction Stress Characteristic Curve (SSCC) related to soil strength is estimated using the relationship between matric suction and volumetric water content.

Chapter 5 shows the results of stability analysis of unsaturated sand slope considering suction stress concept. Based on SSCC, stability analysis of unsaturated sand slope is conducted considering weathering and variation of friction angle at different depth in slope. Futhermore, variation characteristic of factor of safety for slope at different depth is assessed under no infiltration conditions and steady infiltration conditions.

Chapter 6 represents conclusion. All analysis results for unsaturated characteristic of sand and stability of unsaturated sand slope are summarized in this chapter.

Chapter 2. Background

2.1 Matric suction

Water is retained in soil by effect of physical and chemical energy. This energy is typically divided to be in the form of kinetic energy and potential energy. However, kinetic energy in soil is neglected in geotechnical engineering generally, because water flow in soil has slow velocity enough to ignore the velocity head. Therefore, potential energy is the primary component that determines the water condition in soil. As shown in Eq. 2.1, the potential energy is defined as the algebraic sum of the matric potential, osmotic potential, pressure potential and gravitational potential (Campbell, 1988; Or and Wraith, 1999).

$$\Psi_T = \Psi_M + \Psi_O + \Psi_P + \Psi_Z \qquad (2.1)$$

where,

Ψ_T=Total potential

Ψ_M=Matric potential

Ψ_O=Osmotic potential

Ψ_P=Pressure potential

Ψ_Z=Gravitational potential

Matric potential (Ψ_M) is often the largest component of the total potential in unsaturated soils, resulting from combined effects of capillarity and adsorptive forces within the soil. The capillary effect can be explained by surface tension forces at the air-water interface and the adsorptive forces arise primarily from electrical and van der Waals force fields occurring within the vicinity of the soil-water. Osmotic potential (Ψ_O) is the result of dissolved solutes in the pore water and pressure potential (Ψ_P) is the hydrostatic pressure exerted by water above a point. Lastly, gravitational potential (Ψ_Z) is determined by the elevation of the point relative value from an arbitrary reference level. However, in case of typical unsaturated soil, pressure potential is zero, and gravitational potential is also zero as it is a relative value from an arbitrary reference level (Nam et al., 2009).

Therefore, the practical total potential consist of matric potential and osmotic potential. It can be represented as Eq. 2.2.

$$\Psi_T = \Psi_M + \Psi_O = (u_a - u_w) = \Psi_O \tag{2.2}$$

where,

$\Psi_M = (u_a - u_w)$

Matric suction is defined as the pressure difference between the pore air pressure and the pore water pressure. Thus, the value of matric suction is the soil water pressure deficit with respect to air pressure, or the soil water potential deficit with respect to soil water potential at the ambient air pressure. This matric suction is variable by external environment and affects the equilibrium of the soil. Also, osmotic suction according to variation of soil solution effects the structural behavior of soil. However, variation of total suction according to external environment is same as variation of matric suction in the general geotechnical engineering. Therefore, matric suction is mainly considered as the main component of total suction.

2.2 General soil water characteristic curve (SWCC)

Figure 2.1 shows the typical Soil Water Characteristic Curve (SWCC). The horizontal axis can be expressed as gravimetric water content (w), volumetric water content (θ) or effective degree of saturation (S_e). The gravimetric water content is the ratio of the mass of water to mass of soil, and the volumetric water content is the ratio of the volume of water to the total volume. Basic quantities required to establish the SWCC include the saturation water content (θ_s), residual water content (θ_r), and the Air-Entry Value (AEV, Ψ_a). The saturated water content is the maximum volumetric water content of soil when the soil is saturated. The residual water content is the minimum volumetric water content of soil where the water is not expel any more despite large matric suction change. It is only eliminated by heating the soil. The AEV is defined as matric suction where air starts to enter the largest pores in the soil (Fredlund and Xing, 1994). Typically, soil with the finer particle has higher AEV and saturated water content (Nam et al, 2009).

As shown in Fig. 2.1, depending on the magnitude of matric suction, SWCC can be divided into three zones. Within the zone of capillary saturation, matric suction is less than the AEV and within the zone of residual saturation, pore water is retained by molecular bonding mechanism. Within the desaturation zone, pore water is retained in the pore of thin films on the particle surfaces under the influences of solid-liquid interaction mechanism. The amount of water adsorbed within the first two zone is a function of the surface area of the soil particles, the surface charge density of the soil mineral, and the type and valency of any adsorbed exchangeable cations. When the adsorbed films on the particle surface grow thick enough to extend beyond the range of influence of the short-range solid-liquid interaction effects, the characteristic curve enters a regime dominated by capillary pore water retention mechanism. The amount of water adsorbed here is a function of the particle and pore size properties, terminating at the AEV where the capillary air-water interface began to disappear as the system approaches saturation.

The soil typically shows a volumetric water contents that is less for a wetting process than for drying process at a given matric suction. The non-coincidence between drying process and wetting process is defined as hysteresis in the SWCC.

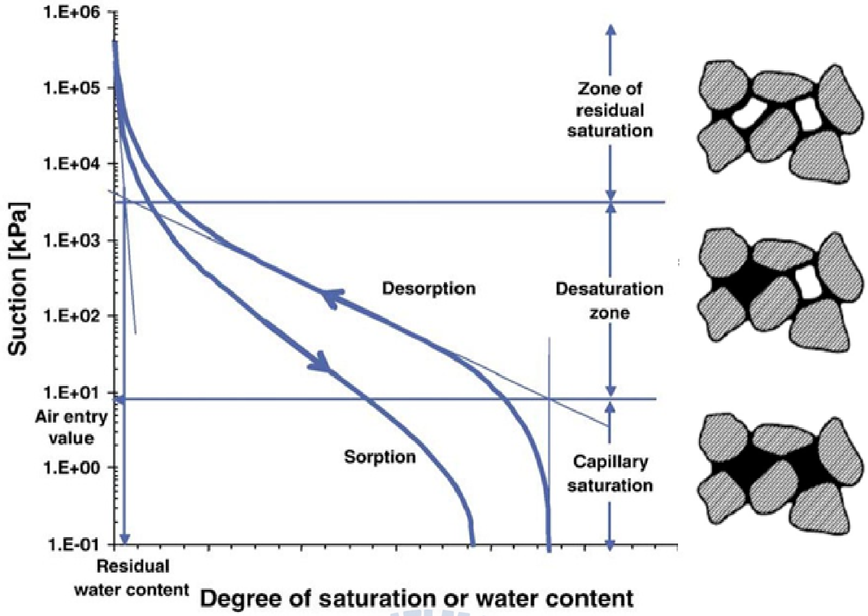

Fig. 2.1 General Soil Water Characteristic Curve

Figure 2.2 shows a typical SWCC for sand, silt, and clay. As shown in figure, AEV and saturated water content (θ_s) are larger in the order of sand, silt and clay. Especially, for sand, variation of water content is relatively larger than others according to variation of matric suction. It is verified that sand has sensitive characteristic according to variation of water content. The water content retained at the each matric suction is affected by capillary effect, pore size distribution and particle size. Therefore, it can evaluate that SWCC is greatly affected by soil structure with particle size.

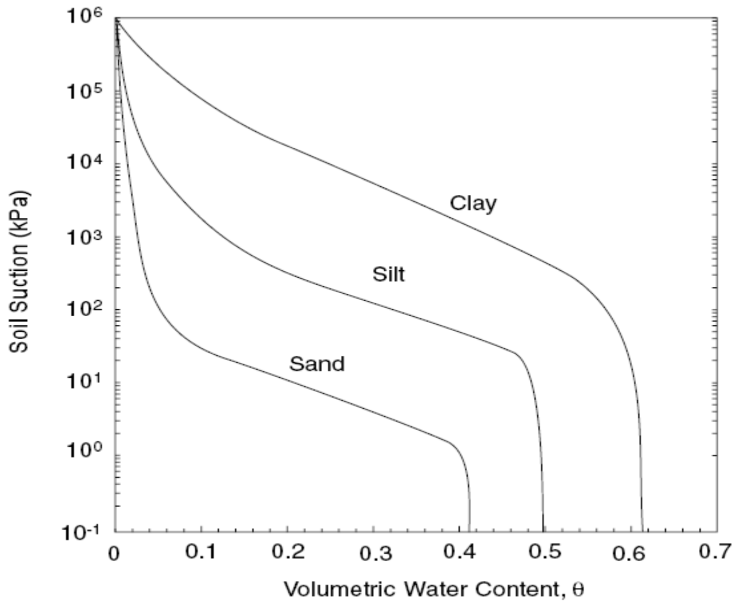

Fig. 2.2 Representative Soil Water Characteristic Curves for sand, silt, and clay (Lu and Likos, 2004)

2.3 Hysteresis

The significant insight into soil-water hysteresis has been gained from both experimental and theoretical perspective (Haines, 1930; Mualem, 1984; Israelachvili, 1992; Nimmo, 1992; Iwata et al., 1995; Lu and Likos, 2004). Hysteretic behavior in SWCC has been attributed to several mechanisms that often referred to as the ink-bottle effect, capillary condensation, entrapped air, swelling and shrinkage, and contact angle hysteresis. Among the several mechanisms, ink-bottle effect and contact angle hysteresis are representative.

Ink-bottle effect in porous media arises due to nonhomogeneity in pore size and shape distribution. As shown in Fig. 2.3, this effect can be understood through analogy by considering the nonuniform capillary tube. The capillary tube is described by two different radii, R being the larger tube radius and r being the smaller tube radius. During upward capillary flow, which is a wetting process, the maximum height of capillary rise h_w is controlled by the smaller tube radius, ceasing at the point where the larger radius is encountered. If the tube is initially filled, which is a drying precess, then the capillary height h_d during drainage may extend beyond the larger pore radius R. Therefore the total water content of the capillary tube during drainage is larger than during wetting.

At many solid-liquid-air interfaces, the wetting solid-liquid contact angle is substantially larger than the drying contact angle. Figure 2.4 shows a classic conceptual example for drop of water on an inclined solid surface. As the drop geometry reaches steady-state under the influence of gravity, a wetting front characterized by relatively large contact angle α_w develops at the advancing edge of the drop. A drying front, which is characterized by a much smaller contact angle α_d, develops at the receding edge. The difference between wetting and drying contact angles in unsaturated soil can be significant. In experimental studies based on capillary rise and horizontal infiltration testing, wetting contact angles in sand can be as high as 60°~80° (Letey et al., 1962; Kumar and Malik, 1990). On the other hand, drying contact angles have been estimated to range from 0° to as much as 20° to 30° less than the corresponding wetting angles (Laroussi and DeBacker, 1979).

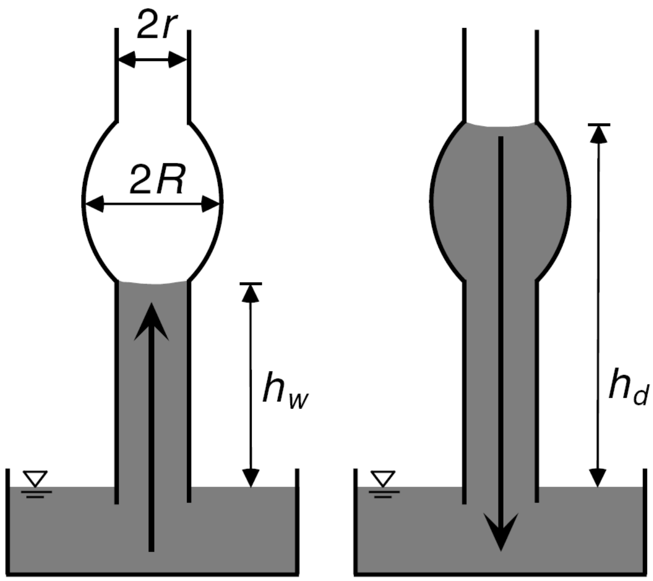

Fig 2.3 Ink-bottle effect (Lu and Likos, 2004)

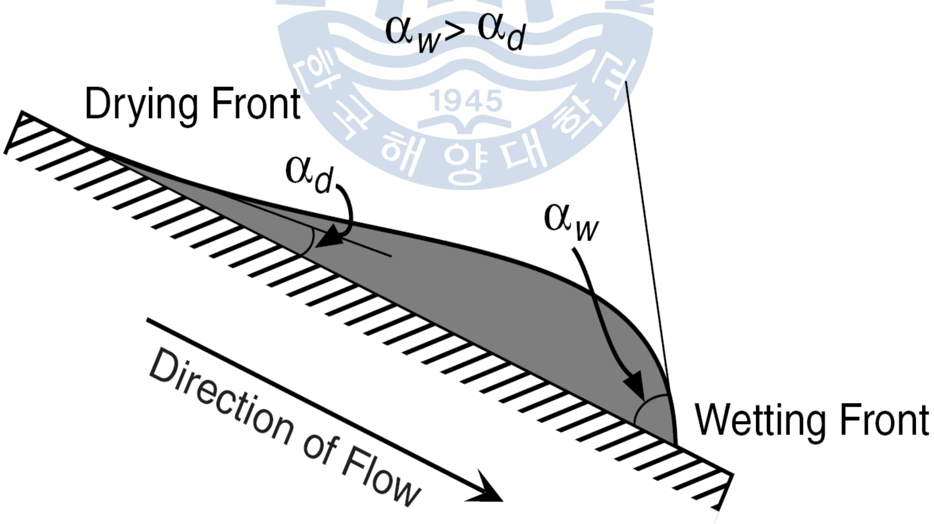

Fig 2.4 Contact angle hysteresis (Lu and Likos, 2004)

Chapter 3. Automated SWCC Experiments

3.1 Composition of test device

Figure 3.1 shows a overall appearance about automated Soil Water Characteristic Curve apparatus (Song et al., 2010). It is composed with combinations of pressure panel, water reservoir, air bubble trap, flowcell, shelf and storage box, balance, and automated soil-water retention system. This apparatus needs to be placed on the flat location without vibration.

Fig. 3.1 Overall appearance of automated SWCC apparatus (Song et al., 2010)

3.1.1 Pressure panel

Pressure panel controls the air pressure supplied by compressor and delivers the controlled air pressure into flowcell. As shown in Fig. 3.2a, Right tube is connected with compressor and left tube is connected with flowcell. So, controlled air pressure is supplied to soil placed on flowcell through the left tube. As shown in Fig. 3.2b, left regulator controls the low air pressure from 0 to 15kPa and right regulator controls the relatively high air pressure from 15kPa to 300kPa. This air pressure acts matric suction (Ψ) of unsaturated soil.

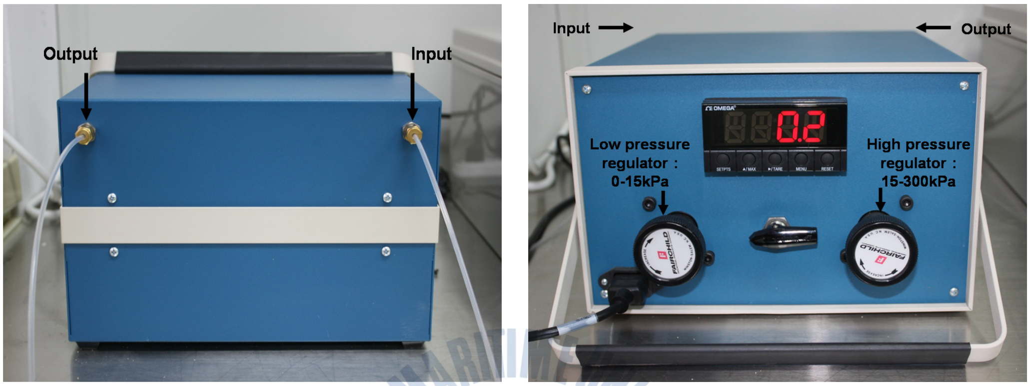

(a) Backside of pressure panel (b) Frontside of pressure panel

Fig. 3.2 Pressure panel

3.1.2 Water reservoir

Water reservoir supplies the water into entire apparatuses with the aim of eliminating the air bubble. As shown in Fig. 3.3b, it is connected with flowcell, air bubble trap, and balance as well as it is higher than the other apparatuses. Therefore, through the difference of head, all apparatuses can be saturated by opening and closing the water reservoir's valves.

(a) Injection of distilled water

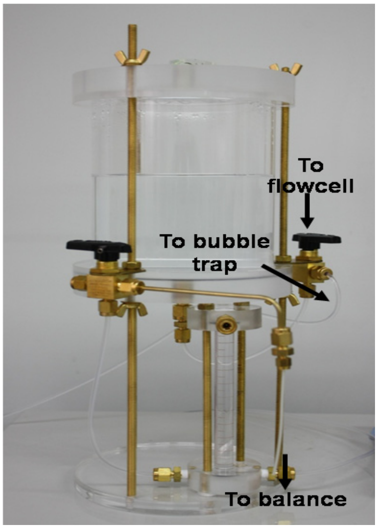

(b) Connection of water reservoir

Fig. 3.3 Water reservoir

3.1.3 Flowcell

Figure 3.4 shows a flowcell which consists of connections of air pressure and air bubble flushing system. The connection of air pressure is connected to pressure panel, and then air bubble flushing system is connected to water reservoir and air bubble trap. As shown in Fig. 3.4(b), saturated soil and HAE (High Air Entry) disk are placed on air bubble flushing system. As a shape of cylinder, soil's diameter is 5.05cm and height is 3.89cm, which is installed by using the plastic mold. Diagram of the air bubble flushing system is shown in Fig. 3.5. Water is injected through the thin tube (1.59mm tube) and air is removed through the tube that connects to the air bubble trap. For the system to work, it is important that water is only injected through the thin tube, so air is not trapped underneath the HAE disk. An O-ring that is placed between the 1.59mm tube and the connector 2 ensures water flow only through the thin tube. The O-ring makes an effective seal when pressed against connector 2 through a spacer tube and connector 3.

(a) Air bubble flushing system

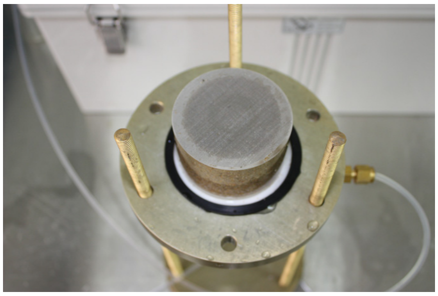

(b) HAE disk and saturated soil

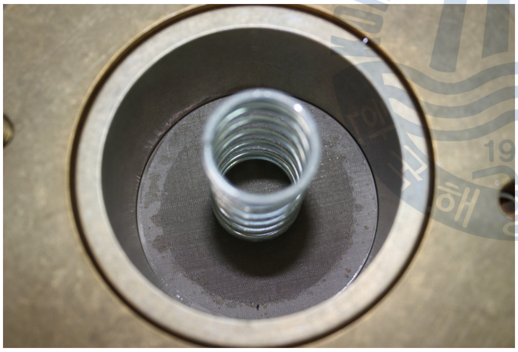

(c) Fixing the soil

(d) Connection of flowcell

Fig. 3.4 Flowcell

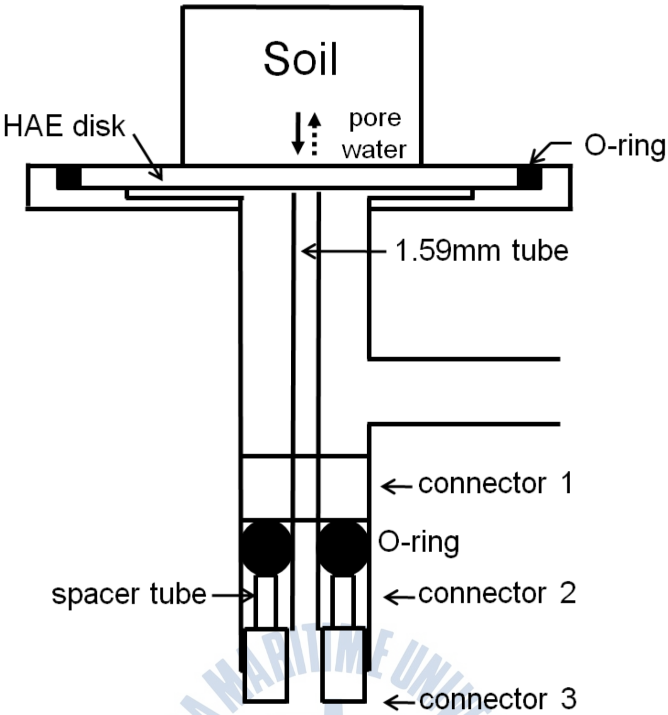

Fig. 3.5 Diagram of the air bubble flushing system

3.1.4 Air bubble trap

The air bubble trap is incorporated into the system to quantify volume of air dissolved through the HAE disk. The air bubble trap has four connections, two on top and two on bottom (Fig. 3.6). The bottom cap is connected to the flowcell on one end, and to the balance on the other end. The top cap is connected to the water reservoir on one end, and can be vented to the atmosphere on the other end.

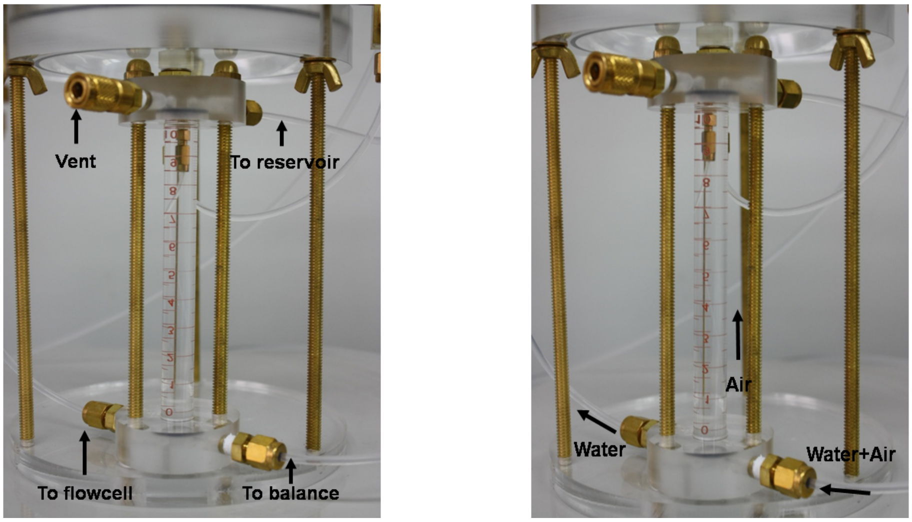

Fig. 3.6 Air bubble trap

3.1.5 Balance

The amount of water that is expelled from the soil sample due to an increase in air pressure is measured on the balance (Fig. 3.7). The balance is then connected to a computer so that all data obtained is recorded automatically from automated soil-water retention system.

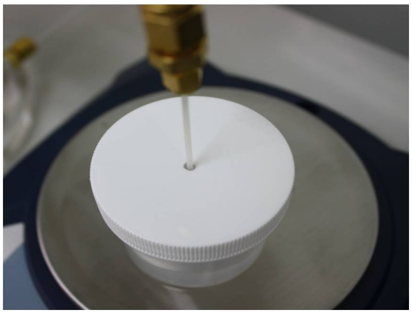

(a) Small reservoir cap

(b) Balance

Fig. 3.7 Measurement apparatus

3.1.6 Automated soil-water retention system

A LabVIEW program allows the user to monitor and control the logging of the data. Figure 3.8 shows the software interfaces which are composed of 10 items.

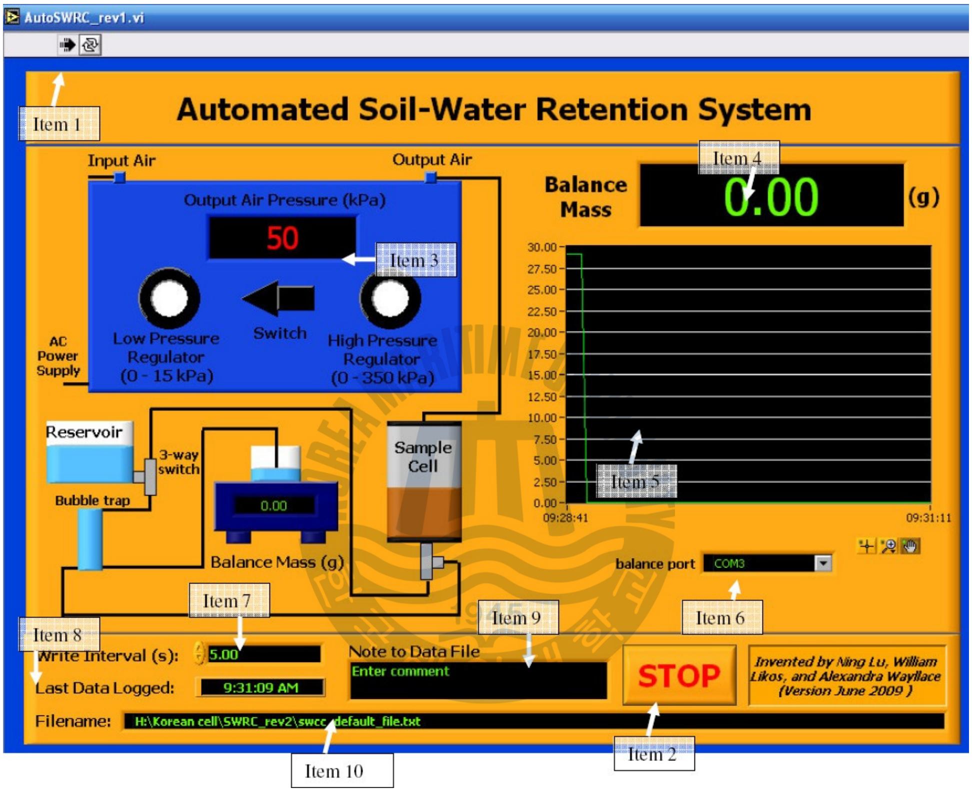

Fig. 3.8 SWRC program

Item 1: Run button. To run the program the "run" arrow must be pressed. If the arrow is filled black, the program is running.

Item 2: Stop button. if the arrow is white, the program has been stop.

Item 3: Output air pressure. Type in the air pressure applied to the soil sample in the window.

Item 4: Balance mass. This window outputs the reading of the balance.

Item 5: This window plots live data of the mass measured by the balance as a function of time.

Item 6: Balance port. The port in the computer used by the balance must be selected in this window.

Item 7: This is write interval. The time unit is seconds.

Item 8: Last data logged. This window displays when the last data point was saved in your data file.

Item 9: Note to data file. Any additional comments can be typed.

Item 10: Filename. This window displays the name and location of data file.

3.2 Principle

Automated SWCC apparatus can simply control the drying process which makes a saturated soil into an unsaturated soil by applying the air pressure, and the wetting process which makes an unsaturated soil into a saturated soil by injecting the water. Therefore, this apparatus can assess comprehensive Soil Water Characteristic Curve (SWCC) of unsaturated soil. Figure 3.9 shows diagram of automated SWCC apparatus. Above all, before conducting the test, all apparatus have to be saturated using water reservoir, because air bubble can cause the error of experimental results during the test process. Then, saturated soil and HAE disk are placed on the air bubble flushing system. After the test preparation is finished, the air pressure supplied from the compressor is controled by pressure panel. This controled air pressure is applied to saturated soil in flowcell. When the air pressure exceeds the AEV of soil, pore water is begin to be expelled, and then it is transferred to the balance through the HAE disk and air bubble trap. In contrast, when the increased air pressure is lowed using the pressure panel, expelled pore water is injected into soil. The applied air pressure and measured the mass of the pore water is available to verification and storage through the SWRC program in real-time, because the balance is associated with a computer. Therefore, automated SWCC apparatus can comprehensively understand the soil-water characteristic of unsaturated soil by conducting the drying process and wetting process. Where, air pressure is acted to matric suction of unsaturated soil, and HAE disk restricts translation of pore air and soil particles excluding pore water.

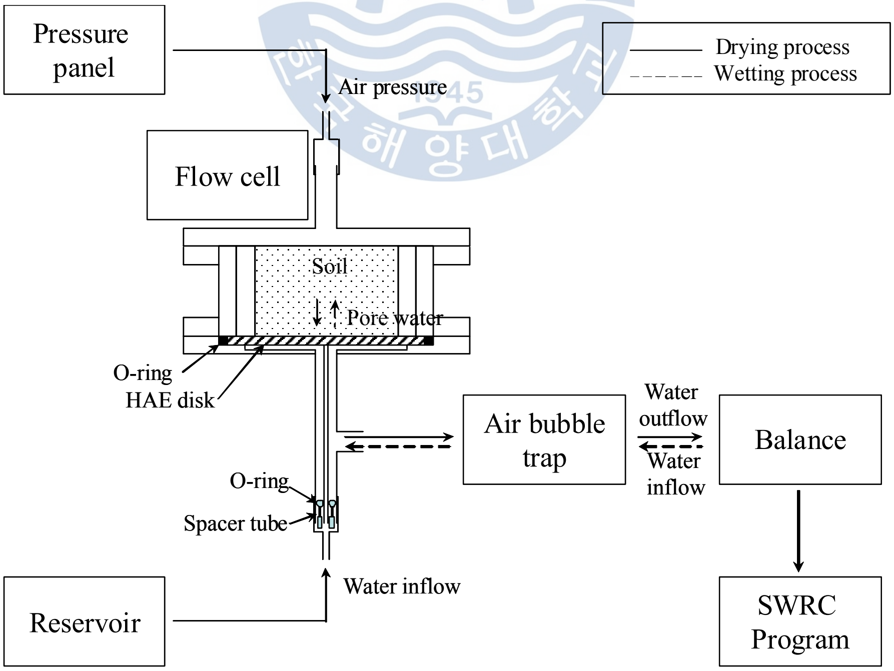

Fig. 3.9 Diagram of automated SWCC apparatus

3.3 Testing preparation

3.3.1 Characteristics of the soil sample

In this study, to understand the characteristic of sand according to density, Joomunjin sand was used as experimental soil sample within the range of relative densities 40%, 60%, and 75%. On the basis of the experimental method of ASTM D 4253-83 and ASTM D 4254-83, maximum dry density and minimum dry density of Joomunjin sand were obtained. Figure 3.10 shows the particle size distribution curve of Joomunjin sand, and Table 3.1 shows the properties of Joomunjin sand.

Table 3.1 Properties of Joomunjin sand

Description	Symbol	Property
Specific gravity	G_s	2.621
Max. void ratio	$e_{\max}$	0.919
Min. void ratio	$e_{\min}$	0.625
Max. dry density	$\gamma_{d\max}$	15.82 kN/m^3
Min. dry density	$\gamma_{d\min}$	13.40 kN/m^3
Effective particle size	D_{10}	0.42 mm
D_{30} particle size	D_{30}	0.51 mm
D_{60} particle size	D_{60}	0.63 mm
Uniformity coefficient	C_u	1.5
Coefficient of curvature	C_c	1.0
Soil classification	USCS	SP

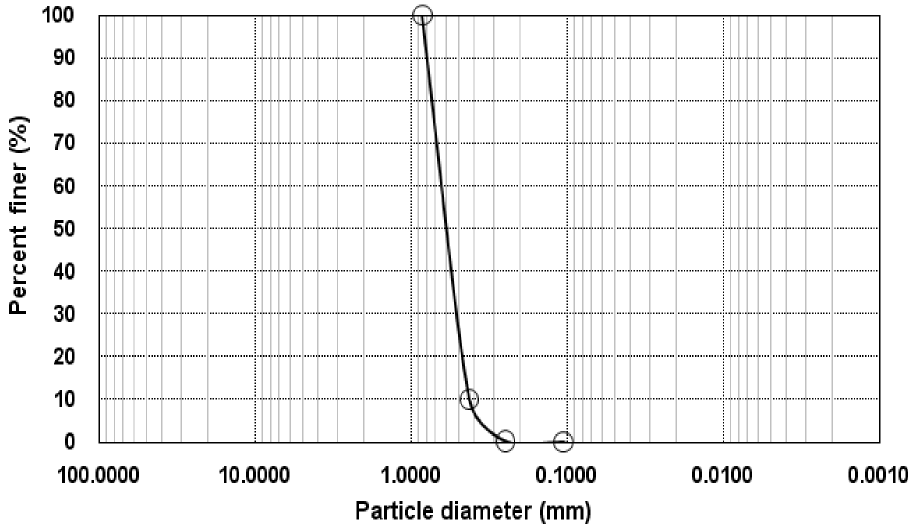

Fig. 3.10 Particle size distribution curve of Joomunjin sand

3.3.2 Saturation of soil and HAE disk

To shape a soil sample, plastic mold in which its diameter is 5.05cm and height is 3.89cm was used. As shown in Fig. 3.11, before saturating the soil, uniformed soil within the range of relative densities 40%, 60%, 75% was made and porous stone was placed at top and bottom of soil sample to effectively flow the water, while saturating the soil. To saturate the soil sample and HAE disk, desiccator and vacuum pump were used. First, distilled water was injected into desiccator and shaped soil was placed in a desiccator where the top 1cm is under vacuum and the rest of the soil is submerged under water. Lastly, inside of desiccator was made into a vacuum by using the vacuum pump to saturate the soil and HAE disk. Therefore, saturation of soil was progressed by flowing the distilled water from bottom to top in soil, while eliminating the air bubble in void of soil. Saturation time is depended on the soil type. For sand, it can get saturated in about 30 minutes. On the other hand, silt and clay should be allowed at least 24 hours.

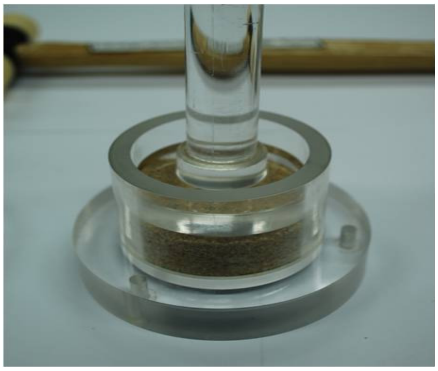

(a) Soil compaction

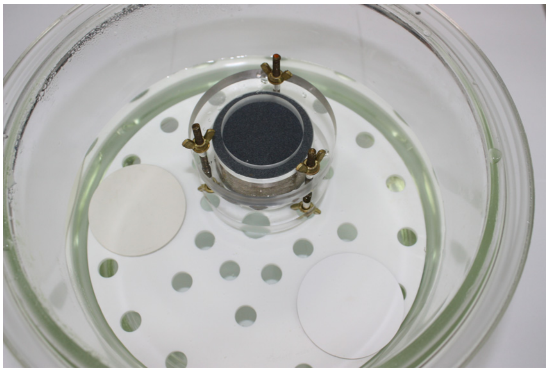

(b) Desiccator

Fig. 3.11 Saturation of soil and HAE disk

Chapter 4. Experimental Results and Analysis

4.1 Soil-water characteristic

As shown in Fig. 4.1, the line shows the mass of water outflow from the soil sample as a function of time. Whereas, the dotted line shows the applied matric suction to soil sample as a function of time. For drying, mass of water out was drastically increased at the beginning according to variation of matric suction step by step, and then mass of water outflow became constant with the passage of the time. In the same manner, For wetting, mass of water outflow was drastically decreased at the beginning according to variation of matric suction step by step and then, mass of water outflow became constant with the passage of the time. Therefore, after confirming the mass of water outflow remained stay at certain levels of matric suction, next level of matric suction was applied.

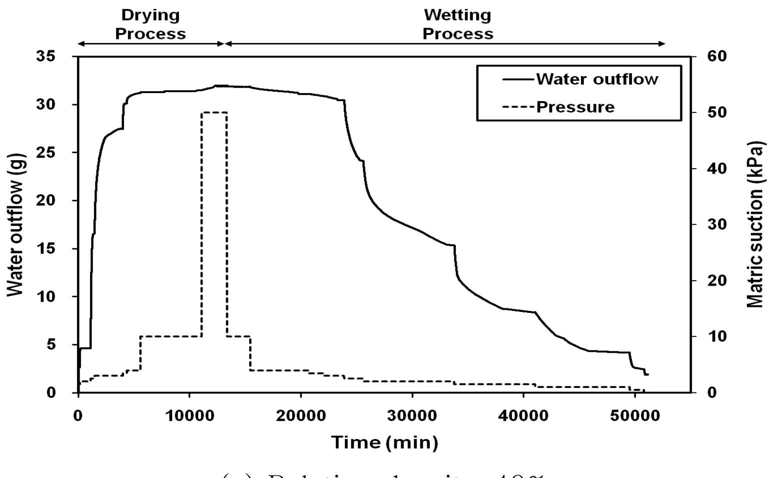

(a) Relative density=40%

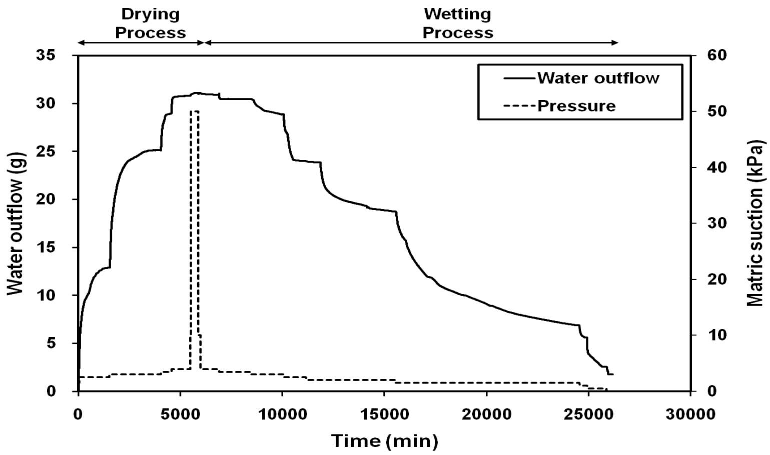

(b) Relative density=60%

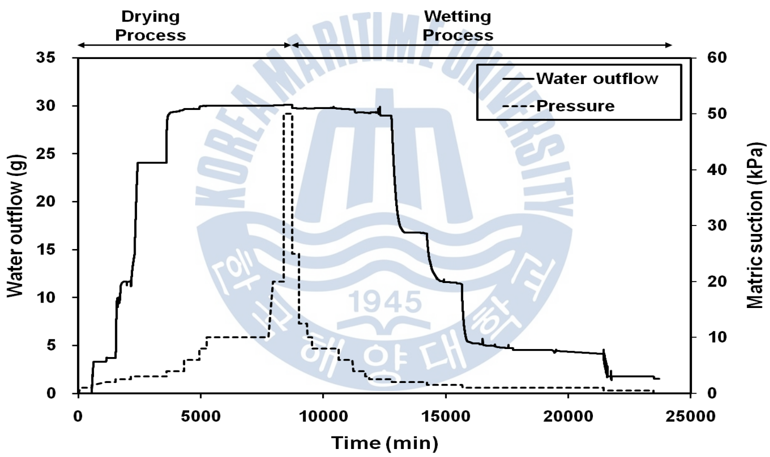

(a) Relative density=75%

Fig. 4.1 Mass of water outflow according to matric suction

Figures 4.2 and 4.3 show the relationship of matric suction and volumetric water contents or effective degree of saturation. As the relative density decreases, the saturated water content is increased. However, residual water contents are almost equal regardless of density. As the results, for sand with the relative density of 40%, it is the highest saturated water content at drying (θ_s=0.44) and wetting (θ_s=0.42). One the other hand, for sand with the relative density of 75%, it is the lowest saturated water content at drying (θ_s=0.41) and wetting (θ_s=0.39). Table 4.1 shows the values of saturated water content and residual water content according to relative density. These values are attributed to difference of soil's pore size and porosity.

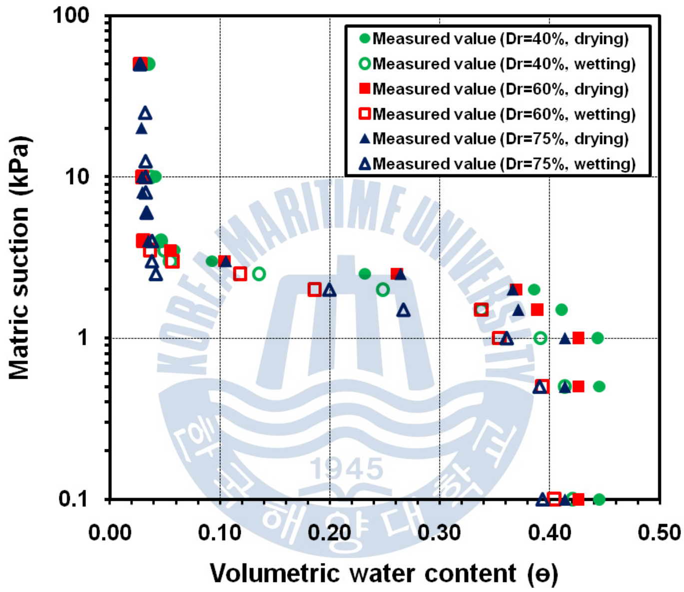

Fig. 4.2 Relationship between matric suction and volumetric water contents

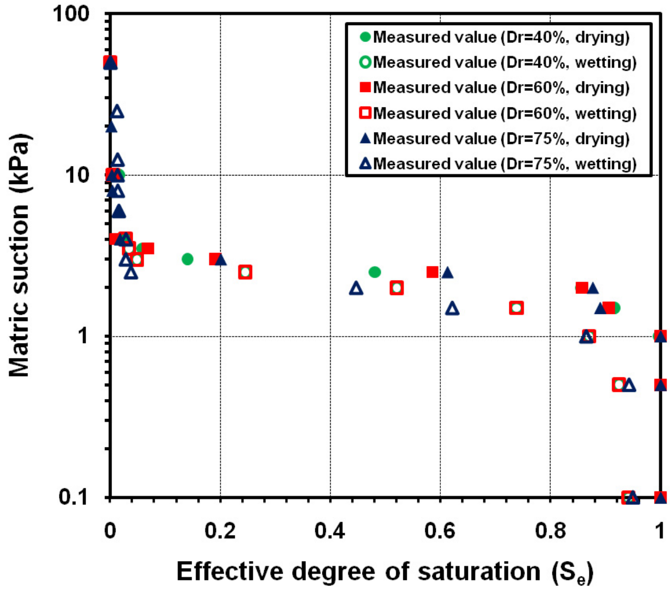

Fig. 4.3 Relationship between matric suction and effective degree of saturation

Table 4.1 The values of saturated and residual water content

	Drying		Wetting	
	θ_s	θ_r	θ_s	θ_r
D_r=75%	0.413	0.028	0.394	0.028
D_r=60%	0.426	0.028	0.404	0.028
D_r=40%	0.445	0.034	0.421	0.034

4.2 Soil water characteristic curve

In estimating the SWCC, numerous models have been proposed for fitting analytical functions through experimental results (Gardner, 1958; Brooks and Corey, 1964; Campbell, 1974; van Genuchten, 1980; Fredlund and Xing, 1994). Among many models, van Genuchten (1980)'s model is most frequently and representatively used to estimate the SWCC. Moreover, it has ability to facilitate closed form analytical solutions for suction stress profiles with a minimum number of parameters.

van Genuchten (1980) proposed the three-parameter equation based on a particular case of the original equation of Mualem (1976). It has shown good results for a variety of soils and is defined as follows

$$S_e = \theta_e = \frac{\theta - \theta_r}{\theta_s - \theta_r} = \left[\frac{1}{1 + [\alpha(u_a - u_w)^n]} \right]^m \tag{4.1}$$

where,

S_e=Effective degree of saturation

θ_e=Effective volumetric water content

θ=Volumetric water content

θ_s=Saturated water content

θ_r=Residual water content

$u_a - u_w$=Matric suction

α=Parameter related to the AEV

n=Parameter related to the slope of SWCC

m=Parameter related to the residual water content

As the α, n, and m are curve fitting parameters, intermediate point (P) between θ_s and θ_r need to be estimated to obtain these parameters. The matric suction corresponding to P is $(u_a - u_w)_p$ and slope corresponding to P is S_p. Thus, curve fitting parameters α, n and m can be obtained by substituting the $(u_a - u_w)_p$ and S_p into Eq. 4.2.

$$\begin{aligned} m &= 1 - \exp(-0.8 S_p) \qquad (0 < S_p \le 1) \\ &= 1 - \frac{0.5755}{S_p} + \frac{0.1}{S_p^{\,2}} + \frac{0.025}{S_p^{\,3}} \qquad (S_p > 1) \end{aligned} \tag{4.2a}$$

$$n = 1/(1-m) \tag{4.2b}$$

$$\alpha = \frac{1}{(u_a - u_w)_p}(2^{1/m} - 1)^{1-m} \tag{4.2c}$$

Table 4.2 shows the values of parameters according to drying and wetting processes. They correspond with range of parameters proposed by Lu et al. (2010). Figures 4.4, 4.5, and 4.6 show the SWCC by van Genuchten's model according to the range of relative density. SWCC shows nonlinear relationship between matric suction and volumetric water content at drying and wetting process (Kim et al., 1996).

Table 4.2 The values of parameters

		a (kPa^{-1})	n	m	AEV (kPa)
D_r=40%	Drying	0.415	8.724	0.855	1.94
	Wetting	0.524	5.625	0.822	
D_r=60%	Drying	0.399	8.586	0.884	2.01
	Wetting	0.548	5.625	0.822	
D_r=75%	Drying	0.393	8.553	0.883	2.10
	Wetting	0.593	5.561	0.820	

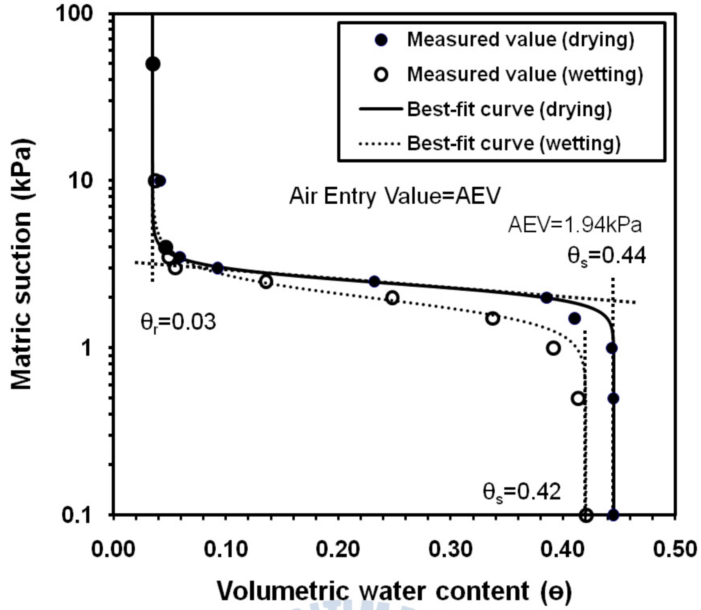

(a) Relationship between matric suction and volumetric water content

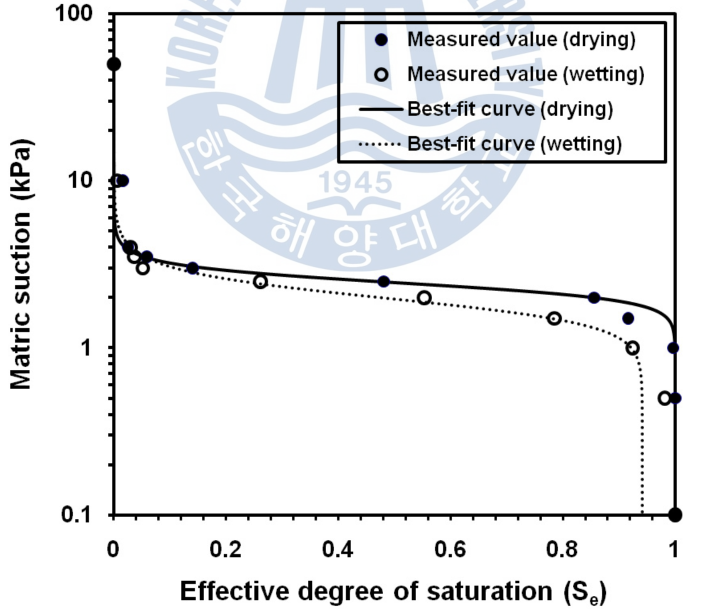

(b) Relationship between matric suction and effective degree of saturation

Fig. 4.4 SWCC by van Genuchten model (D_r=40%)

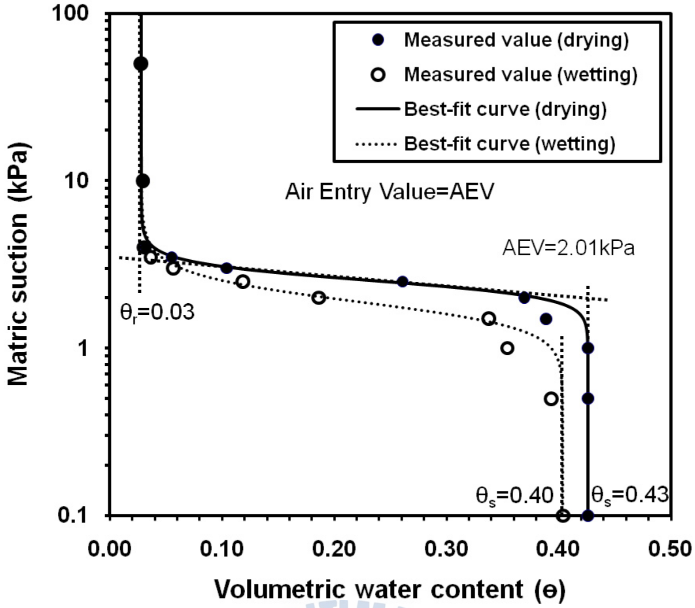

(a) Relationship between matric suction and volumetric water content

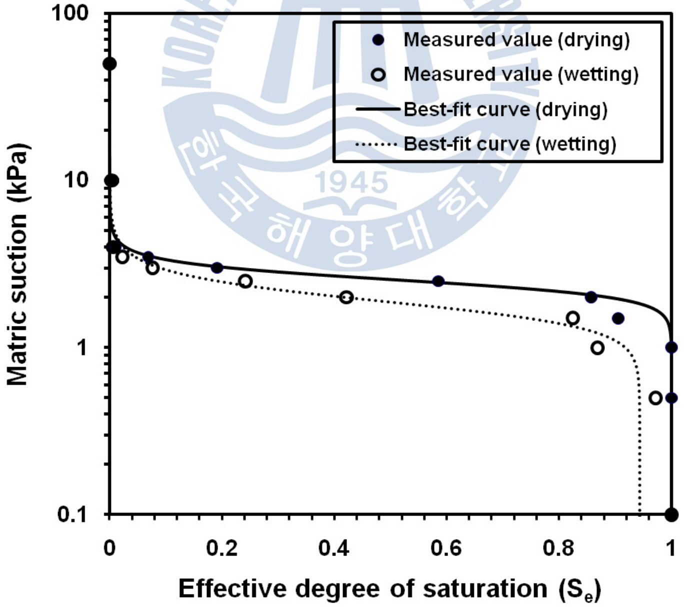

(b) Relationship between matric suction and effective degree of saturation

Fig. 4.5 SWCC by van Genuchten model (D_r=60%)

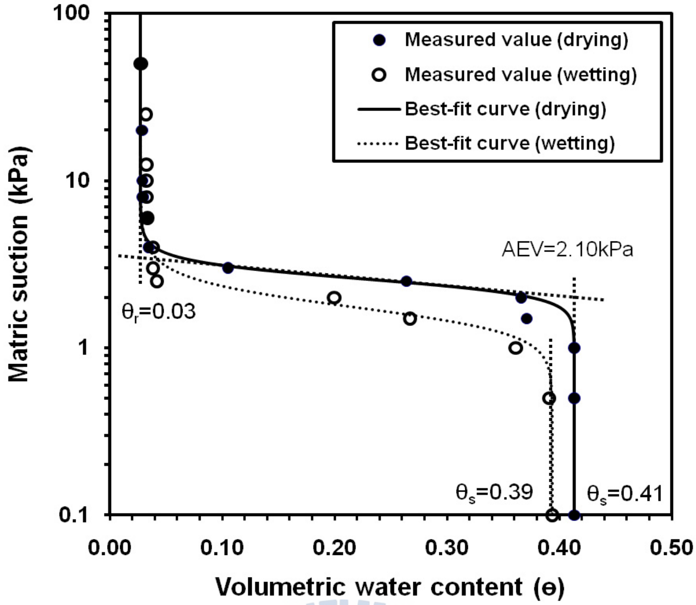

(a) Relationship between matric suction and volumetric water content

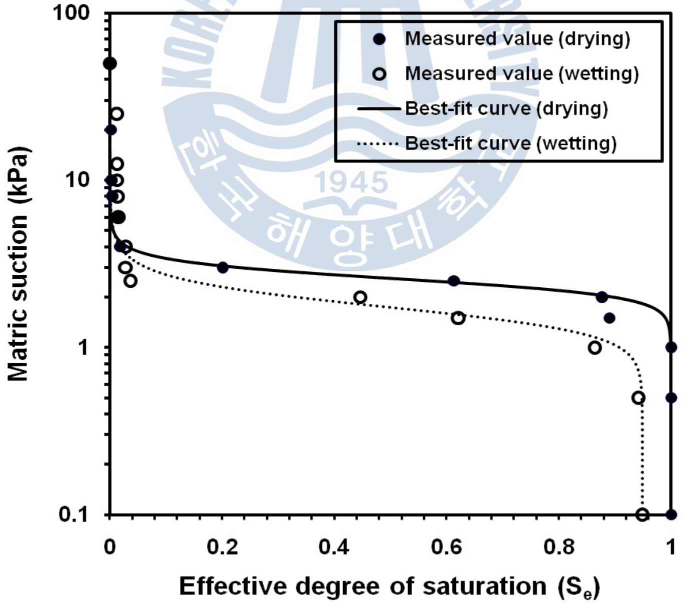

(b) Relationship between matric suction and effective degree of saturation

Fig. 4.6 SWCC by van Genuchten model (D_r=75%)

As the results, for drying, the values of α and n are decreased as relative density is increased. For wetting, the values of α are increased and the values of n are decreased as relative density is increased. If the value of α which has the inverse relationship with AEV is decreased, the value of AEV is increased. Moreover, if the value of n is increased, slope of SWCC is parallel with the horizontal axis.

Therefore, for drying, AEV and variation of volumetric water content under equal variation of matric suction are increased as relative density is increased. Besides, difference of saturated water content (θ_s) between drying and wetting are decreased as relative density is increased. Therefore, difference of hysteresis for SWCC between drying and wetting are decreased as relative density is increased. It is verified by SWCC for drying and wetting as shown in Figs. 4.7 and 4.8.

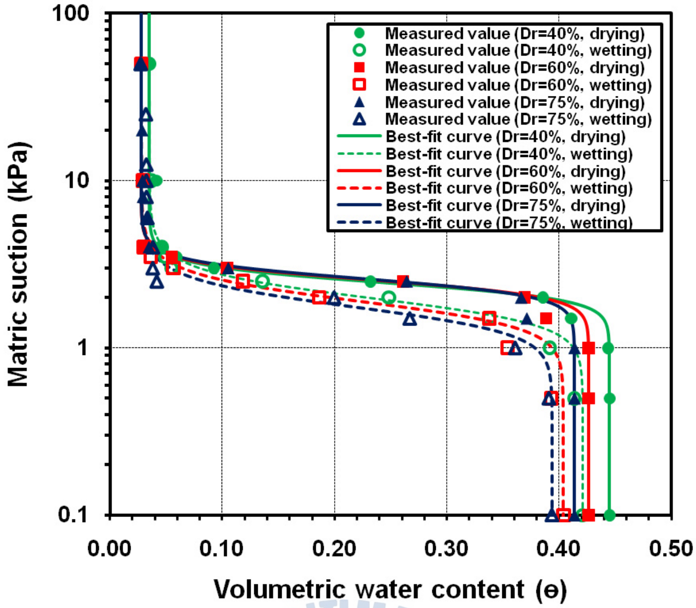

Fig. 4.7 Comparison for SWCC according to relative density (matric suction vs volumetric water content)

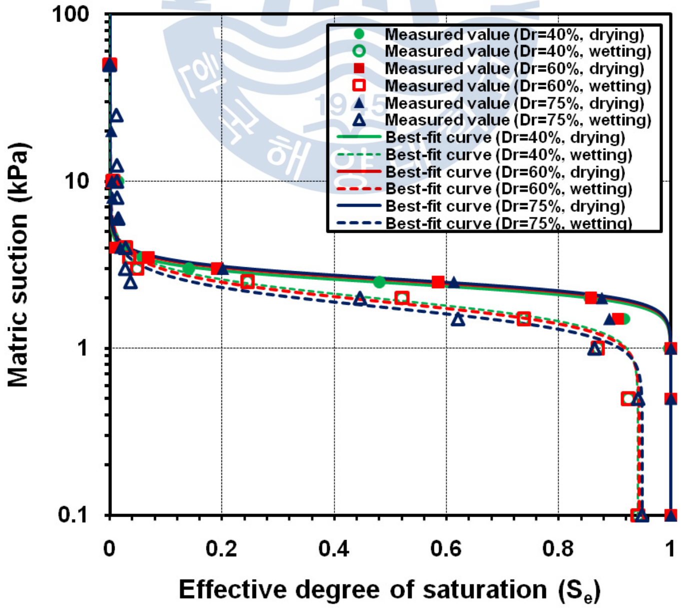

Fig. 4.8 Comparison for SWCC according to relative density (matric suction vs effective degree of saturation)

4.3 Hydraulic Conductivity Function (HCF)

To determine the Hydraulic Conductivity Function (HCF) of unsaturated soil, experimental and theoretical methods have been used. As the experimental methods, steady state method using vertical soil column (Richards, 1931), steady state method using semi-permeable membrane (Hassler and Brunner, 1945) and unsteady state method (Welge, 1952) have been mainly used. As the theoretical methods, parameter estimation method or inverse problem solution technique proposed by many researchers have been mainly used (Zachman et al., 1981; Dane and Hruska, 1983; Abu-Hejleh et al., 1993; Wildenschild et al., 1997). Among these methods, the parameter estimation method which analogizes the hydraulic conductivity function of unsaturated soil through SWCC is the most widely used due to the difficulty of experimatal method. One of the most popular analytical functions for predicting unsaturated hydraulic conductivity of soils is the van Genuchten's parameter estimation method developed by van Genuchten (1980) based on Mualem (1976)'s theory for predicting the k_r from SWCC (Eq. 4.3). This equation is composed of the parameter m or n ($m=1-1/n$). Table 4.3 provides information about saturated hydraulic conductivity according to relative density and Fig. 4.9 shows HCF of sand for drying and wetting according to the range of relative density.

$$k = k_s \times S_e^{\ 1/2}\left[1-(1-S_e^{\ 1/m})^m\right]^2 \qquad (4.3)$$

where,

k=Unsaturated hydraulic conductivity

k_s=Saturated hydraulic conductivity

S_e=Effective degree of saturation

$m=1-1/n\ (0<m<1)$

Table 4.3 Comparison for saturated hydraulic conductivity

Relative density	Saturated hydraulic conductivity, k_s (cm/sec)	
	Drying	Wetting
D_r=40%	2.080E-03	1.583E-03
D_r=60%	1.998E-03	1.539E-03
D_r=75%	1.887E-03	1.482E-03

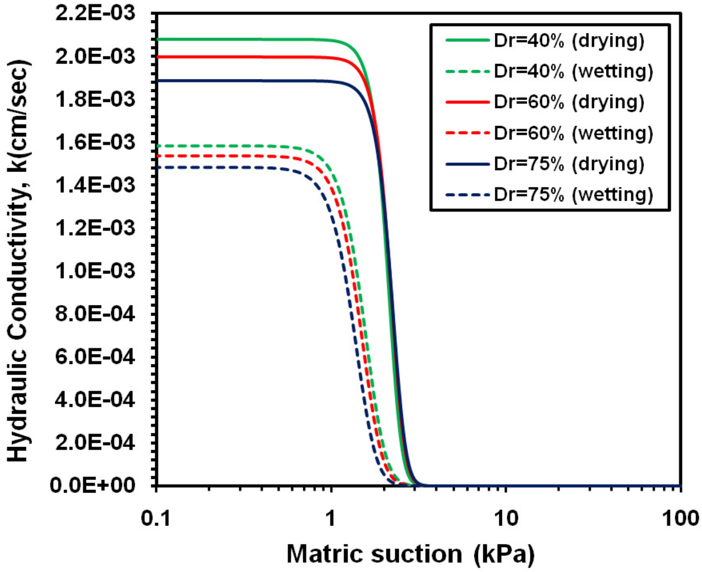

(a) Relationship between hydraulic conductivity and matric suction

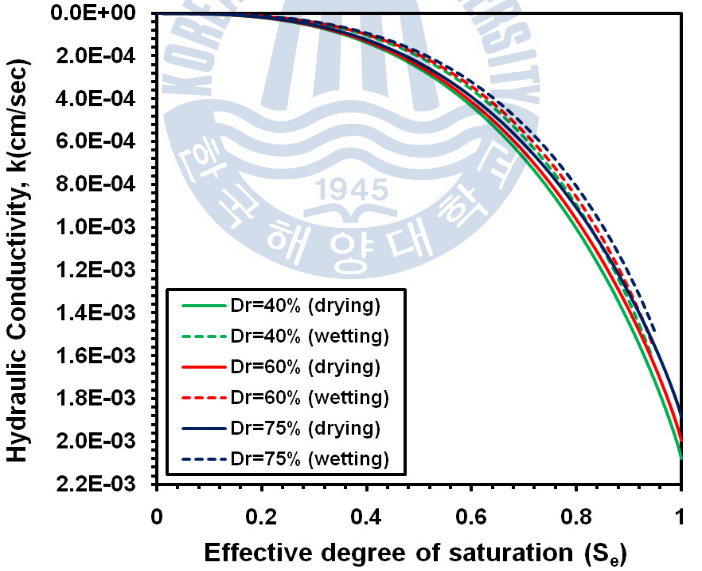

(b) Relationship between hydraulic conductivity and effective degree of saturation

Fig. 4.9 Hydraulic Conductivity Function (HCF)

As the results, hydraulic conductivity is decreased both drying and wetting as matric suction and effective degree of saturation are increased. As relative density increases, hydraulic conductivity is decreased under equal matric suction and effective degree of saturation. Especially, for drying process, variation for hydraulic conductivity is larger than wetting as well as when water flow start to be occurred in soil, the values of matric suction is higher than wetting.

4.4 Suction Stress Characteristic Curve (SSCC)

4.4.1 Existing stress theory of unsaturated soils

There are currently two widely recognized macroscale approaches for describing the state of stress in unsaturated soil. First, the modified effective stress approach, which is generally attributed to the work of Bishop (1959). Second, the independent stress state variable approach, which is generally attributed to the work of Fredlund and Morgenstern (1977).

Bishop's effective stress approach involves a modified form of Terzaghi (1943)'s classic effective stress (Eq. 4.4).

$$\sigma' = \sigma - u_a + \chi(u_a - u_w) \tag{4.4}$$

where,

σ=Total stress

σ'=Effective stress

u_a=Pore air pressure

u_w=Pore water pressure

χ=Effective stress parameter

$(u_a - u_w)$=Matric suction

The effective stress parameter χ is generally considered to vary between zero and one as a function of the degree of pore water saturation.

Following Fredlund and Morgenstern's independent stress state variable approach, net normal stress and matric suction are treated independently in terms of their roles in the mechanical behavior of unsaturated soil. The shear strength by Fredlund and Morgenstern is described as Eq. 4.5. Where, the first two terms comprise the classical Mohr-Coulomb criterion and the third term introduces as an additional friction angle to capture the contribution of matric suction to shear strength.

$$\tau_f = c' + [(\sigma - u_a) + \chi(u_a - u_w)]\tan\phi' \tag{4.5}$$

These two different approaches for describing the state of stress and corresponding behavior of unsaturated soil remain largely uncertain in terms of effectiveness, validity and practicality (Lu and Likos, 2006). In case of Bishop's approach, difficulties associated with experimentally or theoretically determining the effective stress parameter χ have limited the general applicability. Experimental studies have suggested the non-uniqueness of χ=f(S). Also, in case of Fredlund and Morgenstern's approach, similar experimental and conceptual difficulties associated with determining necessary material variables such as ϕ^b and uncertainties in their uniqueness over wide range of saturation have limited the practical applicability of the independent stress variable approach.

Many alternative approaches for stress-strain analyses have been offered in the form of modified stress variables. For example, Matyas and Radhakrishna (1968) explicitly accounted for the contribution of surface tension to intergranular stress. Alonso et al. (1990) expanded the concept of critical state soil mechanics to include volumetric strain due to matric suction. Gallipoli et al. (2003) proposed a stress variable which depends on both the degree of saturation and matric suction for elasto-plastic analysis. Houlsby (1997) illustrated that although the choice of stress state variables for unsaturated soil following phenomenological approaches could be subjective, the strain variables for should be properly identified by the principle of work conjugacy. Identifying the most appropriate and practical approach for conceptualizing and quantifying the state of stress in unsaturated soil and predicting its corresponding macroscopic strength and deformation behavior remains a highly active area of research.

4.4.2 Suction stress for unsaturated soil

In recent, Lu and Likos (2006) introduce theory to represent the state of stress for unsaturated soil as Eq. 4.6. It is an expansion to both

Terzaghi's effective stress for saturated soil and Bishop's effective stress for unsaturated soil.

$$\sigma' = \sigma_t - u_a + \sigma_{pc} + \sigma_{cap} + \chi(u_a - u_w) \tag{4.6}$$

where,

$\sigma_t - u_a$=Net normal stress

σ_{pc}=Interparticle physicochemical stress

σ_{cap}=Capillary stress due to surface tension.

As shown in Eq. 4.6, assuming that interparticle physicochemical stress and capillary stress are eliminated, effective stress proposed by Lu and Likos is equal to expand Bishop's approach.

Suction stress (σ^s) is conceptualized as Eq. 4.7. Where, F_{pc} is interparticle physicochemical force and F_{cap} is capillary force arising from surface tension.

$$\sigma^s = \sigma_{pc} + \sigma_{cap} + \chi(u_a - u_w) = \frac{F_{pc}}{A} + \frac{F_{cap}}{A} + \chi(u_a - u_w) \tag{4.7}$$

As shown in Eq. 4.8, it is the resultant of interparticle physicochemical stresses attributable to cementation σ_{ce}, van der Waals attraction σ_{vdw}, double-layer repulsion σ_{edl}.

$$\sigma_{pc} = \sigma_{ce} + \sigma_{vdw} + \sigma_{edl} \tag{4.8}$$

Thus, effective stress is estimated by introducing suction stress and considering a variety of states arising from unsaturated soil. As the results, suction stress can be used as an index which assesses the state of stress for unsaturated soil, because it has closed relationship between matric suction and degree of saturation. The effective stress of unsaturated soil can be arrived as Eq. 4.9 by reorganizing suction stress shown in Eq. 4.6 (Lu and Likos, 2006).

$$\sigma' = (\sigma - u_a) - \sigma^s = (\sigma - u_a) + (u_a - u_w)S_e \tag{4.9}$$

where,

$\sigma^s = -(u_a - u_w)S_e$

S_e = Effective degree of saturation

As shown in Eq. 4.9, suction stress is expressed as a negative (-) value and it can be considered as the effective stress under no external stress condition. Therefore, it is important to be considered in determining the strength of unsaturated soil. Moreover, the graphic representation of suction stress is the area under the normalized SWCC. Thus, suction stress has closed relationship with SWCC. This relationship between suction stress and matric suction or effective degree of saturation is defined as Suction Stress Characteristic Curve (SSCC) which can estimate and predict the strength of unsaturated soil according to water content (Lu and Likos, 2006; Lu et al., 2010).

Figure 4.10 shows the relationship between SWCC and SSCC. The van

Genuchten's parameters of SWCC can be used to determine the SSCC according to effective degree of saturation by Eq. 4.10, and effective water content by Eq. 4.11. A closed-form equation of suction stress for the full range of saturation can be arrived at by substituting Eq. 4.1 into Eq. 4.9.

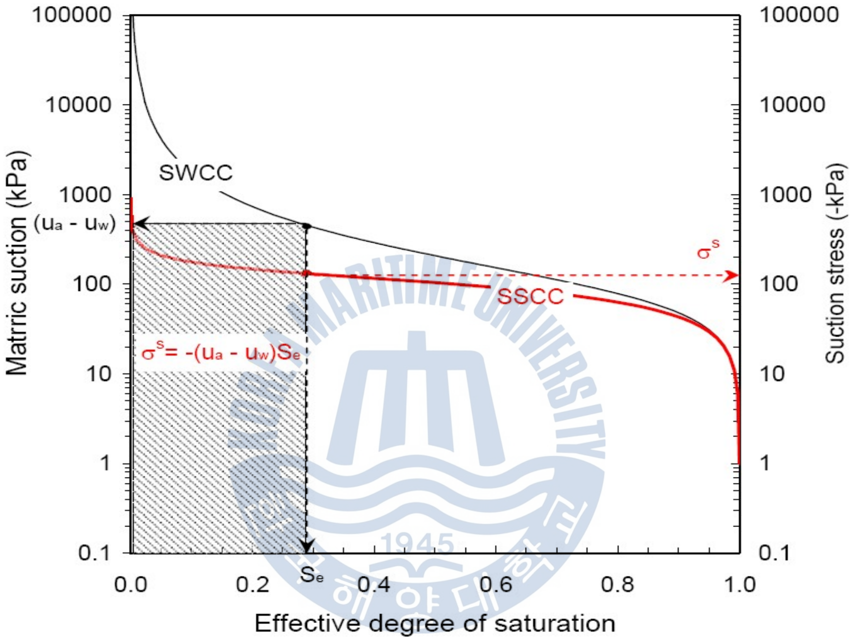

Fig. 4.10 Relationship between SWCC and SSCC (Lu and Godt, 2008)

(Relationship between suction stress and effective degree of saturation)

$$\sigma^s = -\frac{S_e}{\alpha}\left(S_e^{\frac{n}{1-n}} - 1\right)^{\frac{1}{n}} \qquad 0 \le S_e \le 1.0 \qquad (4.10)$$

(Relationship between suction stress and matric suction)

$$\sigma^s = -(u_a - u_w) \qquad u_a - u_w \le 0 \qquad (4.11a)$$

$$\sigma^s = -\frac{(u_a - u_w)}{(1+[\alpha(u_a - u_w)]^n)^{(n-1)/n}} \qquad u_a - u_w > 0 \qquad (4.11b)$$

4.4.3 Comparison and analysis for suction stress of sands

Figure 4.11 shows the SSCC for sand with the range of relative densities using fitting parameters (α, n). As the results, suction stress has increased-and-decreased characteristic along with increasing matric suction as well as maximum suction stress is showed at AEV (Ψ_a). Moreover, suction stress is zero at zero matric suction (saturated condition) and at value of matric suction more than about 8kPa (pendular zone). For drying process, maximum suction stress is increased as relative density increases. However, for wetting process, maximum suction stress is increased as relative density increases. Table 4.4 shows the values of maximum suction stress for unsaturated sand with the range of relative densities.

This behavior of maximum suction stress is well-known for sand-sized granular media (Schubert, 1975; Kim, 2001; Lu et al., 2007). A practical illustration of such mechanical behavior is the building of sandcastles. If the sand is too dry or too wet, the sand cannot be used to build a structurally sound sandcastle. It is important that this behavior cannot be effectively described using Bishop's effective stress approach.

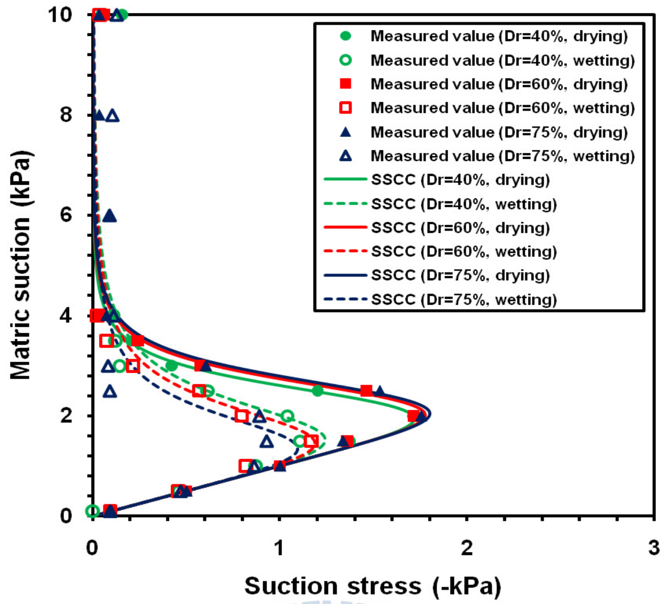

(a) Relationship between suction stress and matric suction

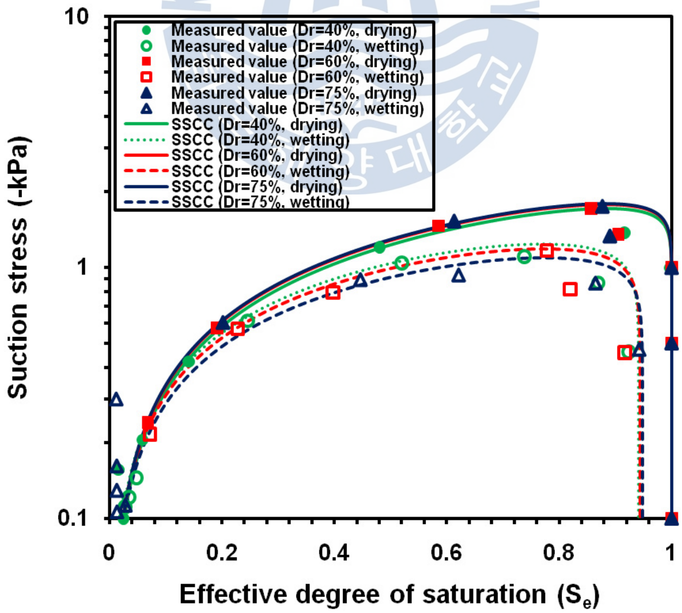

(b) Relationship between suction stress and effective degree of saturation

Fig. 4.11 Comparison for SSCC according to relative density

Table 4.4 The values of maximum suction stress

		Ψ_a (kPa)	S_e	$\sigma^s{}_{\max}$ (-)
Drying	D_r=40%	1.94	0.88	1.71
	D_r=60%	2.01	0.88	1.78
	D_r=75%	2.10	0.88	1.80
Wetting	D_r=40%	1.52	0.77	1.24
	D_r=60%	1.45	0.77	1.19
	D_r=75%	1.34	0.77	1.10

Figure 4.12 illustrates the relationship for SSCC and state of suction stress at saturation, $\sigma^s = -(u_a - u_w)$. Once the matric suction reaches and exceeds the soil's AEV, suction stress of sand is rapidly decreased Therefore, after matric suction exceeds AEV, effective stress of unsaturated soil has difference value compared to saturated soil.

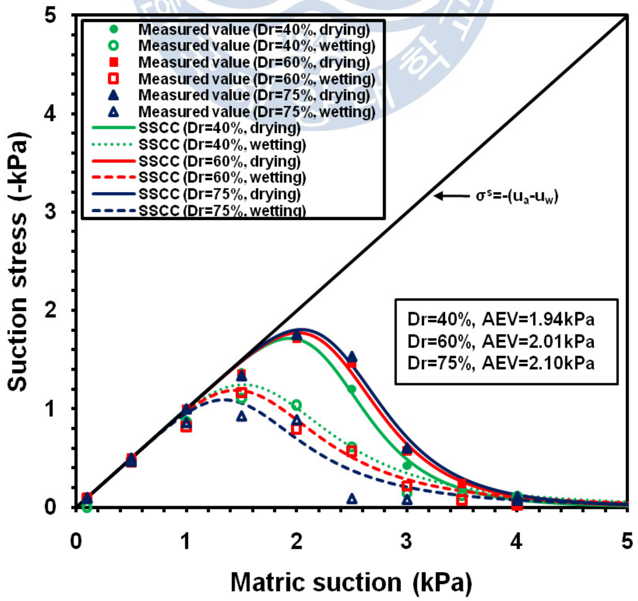

Fig. 4.12 Relationship between SSCC and suction stress at saturation

Chapter 5. Stability Analysis of Unsaturated Sand Slope

5.1 Theories

The stability of natural and engineered earthen slope is a classical subject in soil mechanics, slope hydrology, and geomorphology (Lu and Godt, 2008). Until recently, most slope-stability analyses have been based on Terzaghi (1943)'s effective stress principle in which pore water pressure is quantified by saturated seepage theories (Cho, 2000). However, in well-drained colluvial soils, shallow slope failures may occur within the vadose zone under partially saturated soil conditions (Wolle and Hachich, 1989; de Campos et al., 1991; Godt et al., 2006).

When the moisture variation in the vertical direction in hillslope is important, the consequent effective stress above the water table may need to be considered rigorously. The effective stress in partially saturated soil is no longer the difference between the total stress and pore-water pressure or soil suction. The generalized effective stress which unifies both saturated and unsaturated conditions has been proposed by Lu and Likos (2004, 2006).

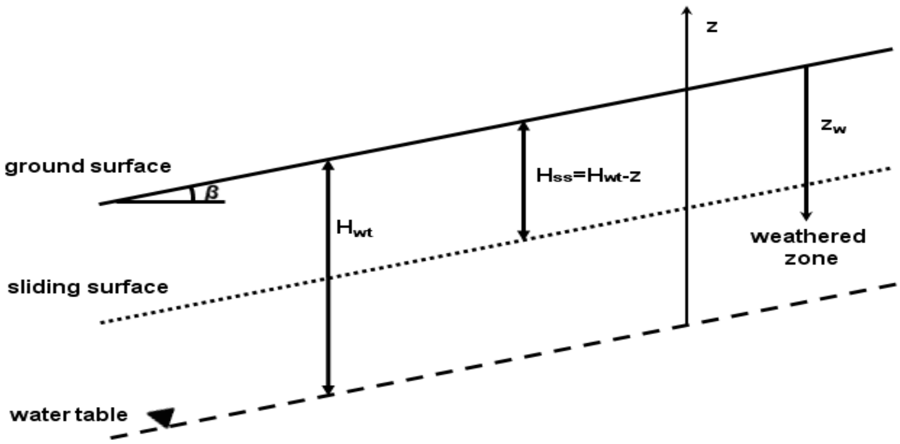

Fig. 5.1 General infinite slope

where,

z=Distance above water table

z_w=Weathering zone

β=Slope angle

For the factor of safety under partially saturated conditions, the general equation for factor of safety of slope is represented as shown in Eq. 5.1.

$$F = \frac{\tau_f}{\tau} = \frac{c' + \sigma' \tan\phi'}{\gamma H_{ss} \sin\beta \cos\beta} \tag{5.1}$$

The effective stress (Eq. 4.9) considering suction stress can be inserted into Eq. 5.1 for infinite slope stability.

$$F = \frac{c' + [\gamma H_{ss} \cos^2\beta - \sigma^s] \tan\phi'}{\gamma H_{ss} \sin\beta \cos\beta} = \frac{\tan\phi'}{\tan\beta} + \frac{2c'}{\gamma H_{ss} \sin 2\beta} - \frac{\sigma^s}{\gamma H_{ss}} (\tan\beta + \cot\beta) \tan\phi' \tag{5.2}$$

The first term on the right side is represented as the internal frictional resistance of the soil. The second term is represented as cohesion, and the third term is represented as the suction stress. Suction stress is greatly reduced as soils near saturation, and this phenomenon could be the physical mechanism triggering many shallow landslides, when hillslopes are subjected to intense precipitation. Therefore, Eq. 5.2 can be used to assess the impact of soil properties and infiltration conditions on the stability of an infinite slope (Lu and Godt, 2008).

In the general infinite slope theory, if the type of soil is uniform, the friction angle (ϕ') is constant regardless of depth. However, for soils with the same chemical composition, soil porosity at the ground surface is typically greater than at the deeper locations. Therefore, since soil porosity (n) is different depending on the depth of the slope, friction angle (ϕ') is affected depending on the depth of the slope. Experimental evidence shows that the friction angle for a sand can vary from 30° to 55° and is inversely linearly proportional to its porosity (Rowe, 1969; Mariachi et al., 1969; Conrforth, 1973; Cornforth, 2005). Thus, such dependency can be mathematically described as shown in Eq. 5.3.

$$\phi = \phi_o + \frac{\Delta\phi}{\Delta n}(n_o - n) \tag{5.3}$$

where,

ϕ_o=Friction angle at the ground

n_o=Porosity at the ground

$\Delta\phi$=Range of variation in friction angle within the weathering zone

Δn=Range of variation in porosity within the weathering zone

Reduction of porosity according to depth is mainly a result of compaction and consolidation under the soil's self weight or external loadings. The functional relationship between porosity and soil depth (H_{ss}) can be described as shown in Eq. 5.4.

$$n = n_o - \frac{\Delta n}{1 + \frac{z_w}{H_{ss}}} \tag{5.4}$$

Equation for friction angle depending on depth of slope (Eq. 5.5) can be arrived by substituting Eq. 5.4 into Eq. 5.3. Figure 5.2 shows the relative change in friction angle as a function of soil depth for various weathering zone parameters (z_w=0.2m, 0.5m, 1.0m).

$$\phi = \phi_o + \frac{\Delta\phi}{1 + \frac{z_w}{H_{ss}}} \tag{5.5}$$

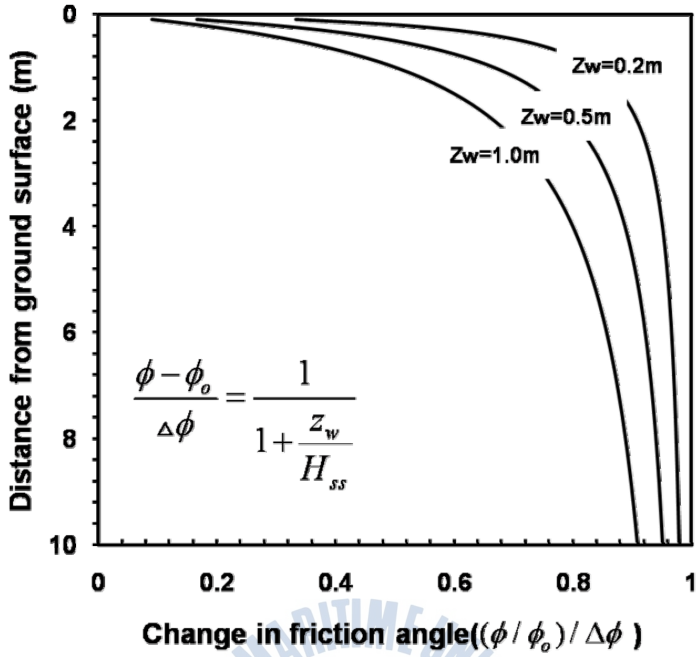

Fig. 5.2 Variation in friction angle following weathered zone depth

With the above conceptualization of a weathered soil, a generalized factor of safety equation both saturated and unsaturated conditions is described as shown in Eq. 5.5. With the seepage rate (q), the soil's hydrologic properties (α, n, k_s), shear strength parameters (c', ϕ'), and weathering characteristics ($\Delta\phi'$, z_w), Eq. 5.6 can be readily used to assess the stability of unsaturated infinite slopes.

$$F(z) = \frac{\tan\phi'(z)}{\tan\beta} + \frac{2c'}{\gamma(H_{wt} - z)\sin 2\beta} - r_u(\tan\beta + \cot\beta)\tan\phi'(z)$$

$$r_u = \frac{\sigma^s}{\gamma(H_{wt} - z)} \quad , \quad \phi(z)' = \phi_o + \frac{\Delta\phi}{1 + \frac{z_w}{H_{ss}}} \qquad (5.6)$$

The matric suction or suction stress generally varies within a slope, depending on soil types, location of water table and slope configuration, and infiltration condition. For a one-dimensional steady state matric suction profile, the matric suction on all these afore mentioned factors can be expressed as shown in Eq. 5.7 (Lu and Griffiths, 2004).

$$u_a - u_w = -\frac{1}{\alpha}\ln[(1+q/k_s)e^{-\gamma_w \alpha z} - q/k_s] \tag{5.7}$$

where,

q=Steady infiltration rate (-) or steady evaporation rate (+)
k_s=Saturated hydraulic conductivity
γ_w=Unit weight of water
z=Vertical coordinate upward positive

The equation for suction stress under steady infiltration or steady evaporation conditions can be leaded by substituting Eq. 4.1 and Eq. 5.7 into Eq. 4.9.

$$\sigma^s = -(u_a - u_w) \tag{5.8a}$$

$$\sigma^s = \frac{1}{\alpha}\frac{\ln[(1+q/k_s)e^{-\gamma_w \alpha z} - q/k_s]}{\left(1+\left\{-\ln[(1+q/k_s)e^{-\gamma_w \alpha z} - q/k_s]\right\}^n\right)^{(n-1)/n}} \tag{5.8b}$$

When the flow rate is equal to zero, the Eq. 5.8b recover to an analytical equation of SSCC (Eq. 4.11). This equation provides a way to expand the classical infinite slope model for unsaturated condition.

5.2 Conditions of sand slope

As shown in Fig. 5.1, to assess the stability of unsaturated infinite slope existing water table, slope is assumed that it is composed of sand within the range of relative densities 40%, 60%, and 75%, respectively. Table 5.1 shows the conditions of infinite sand slopes.

Table 5.1 Conditions of sand slopes

Direct shear test	ϕ_o (°)	D_r=40%	37.54
		D_r=60%	39.98
		D_r=75%	43.27
Slope conditions	$\Delta\phi$ (°)		6
	β (°)		45
	H_{wt} (m)		5
	z_w (m)		0.5

As shown in Table 5.1, infinite slope is assumed that it is composed of sand (D_r=40°, 60°, 75°) and it's gradient is 45°. Moreover, range of variation in friction angle within the weathering zone is assumed to be 6° (Lu and Godt, 2008). Also, parameters (α, n) are equal to SWCC parameters. As the results of direct shear test, values of friction angle are increased along with increasing relative density and value of cohesion is zero regardless of relative density. In this study, to assess the stability of sand slope according to variation characteristic of water content, water table was considered from ground below 5m and stability analysis was conducted under no infiltration conditions and steady infiltration conditions.

5.3 Under no infiltration

Suction stress in sand under hydrostatic equilibrium conditions can be assessed by Eq. 4.11 for three sands according to relative density. For no infiltration condition, factor of safety according to drying and wetting process at different depths in sand slope is shown in Fig. 5.3.

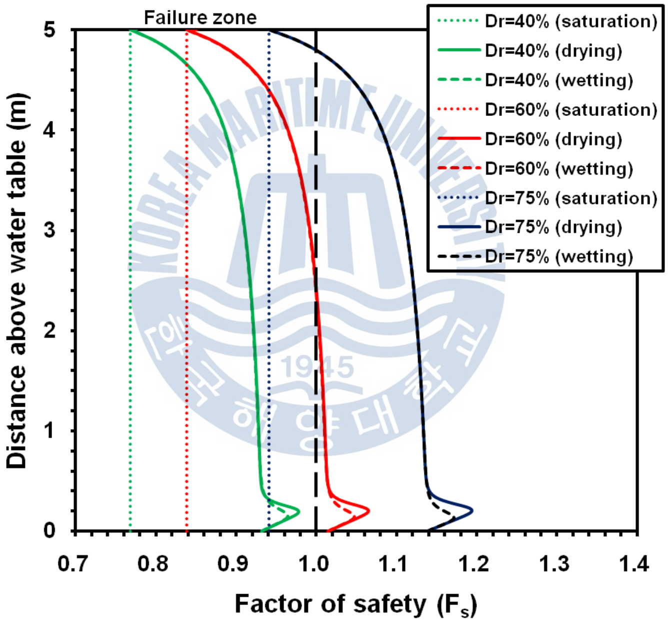

Fig. 5.3 Analysis for factor of safety under no infiltration condition

For slope with relative densities of 60% and 75% sands, the factor of safety (F_s) reaches 1 at about 2.4m and 4.8m above the water table. Therefore, these two sand slopes inclined at 45° will not be stable if the unsaturated zone is thicker than 2.4m and 4.8m respectively. For slope with relative density of 40% sands, the factor of safety is less than 1 in all the depth.

In the three sand slopes, the variation of the factor of safety shows the four distinct zone ; the zone of sharp increasement between 0 to 0.2m above water table, the zone of sharp reduction between 0.2m to 0.4m above water table, the zone of gradual reduction between 0.4m to 4.0m, and the zone of increasingly sharp reduction is within 1m to the ground surface due to decrease of friction angle by weathering. The two zones of sharp increasement and sharp reduction between 0 to 0.4m are affected by suction stress and the other two zones are affected by friction angle.

For these sand slopes, maximum suction stress ($\sigma^s_{\max}$) is occurred at the location of sand's Air Entry Value (AEV, Ψ_a), and the maximum factor of safety ($F_{s\max}$) nearly accord with the location of the maximum suction stress. As the results, the maximum factors of safety about drying are 0.98, 1.06, and 1.19 respectively. In the same way, for wetting, maximum factors of safety are 0.96, 1.05, and 1.14 respectively.

If the slope exists on the full saturated state, effect for weathering and suction stress is not occurred in slope. Therefore, stability of slope are decided only slope angle and friction angle. As the results, factor of safety of sand slope under saturated state shows linear pattern regardless of slope depth and exist more unstable than unsaturated state.

5.4 Under steady infiltration rate

For steady infiltration conditions, predicted slope failure in unsaturated ground can be assessed by Eq. 5.7. To assess the factor of safety at different depths in sand slope, saturated hydraulic conductivity (k_s) according to relative density has to be measured through the water permeability tests previously.

In this study, steady infiltration rates are assumed as -1.0×10^{-3}cm/s, -1.5×10^{-3}cm/s, and -1.8×10^{-3}cm/s. Such series of infiltration rates represent very heavy rainfall intensity which is realistically impossible. However, in this study, infiltration rates are considered theoretically, because Joomunjin sand has high saturated hydraulic conductivity. By mathematical definition, the infiltration rate q should be less or equal to the saturated hydraulic conductivity. Figures 5.4, 5.5, and 5.6 show the volumetric water content and suction stress according to distance above water table under assumed steady infiltration rates.

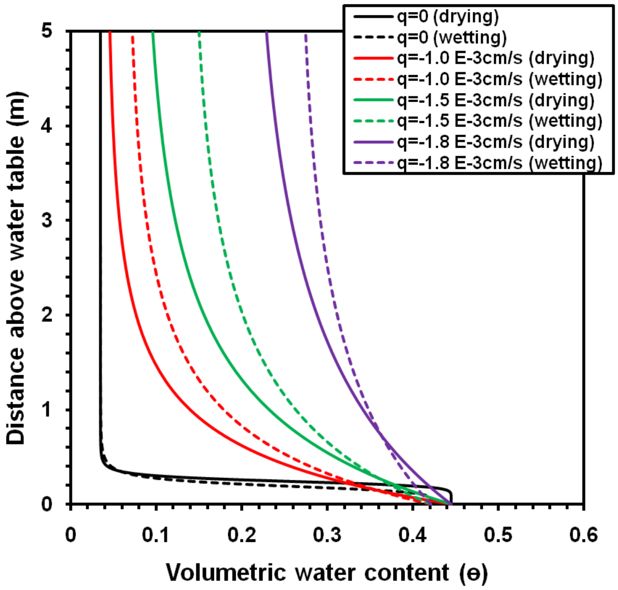

(a) Relationship of distance above water table vs volumetric water content

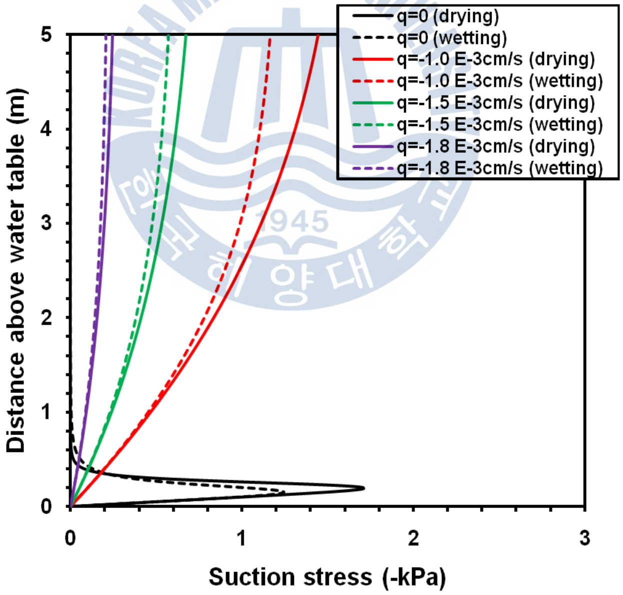

(b) Relationship of distance above water table vs suction stress

Fig. 5.4 Variation for matric suction and suction stress under steady infiltration rates (D_r=40%)

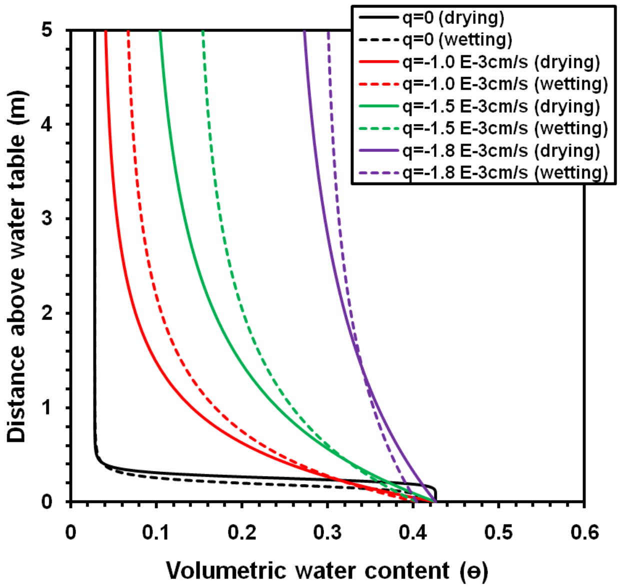

(a) Relationship of distance above water table vs volumetric water content

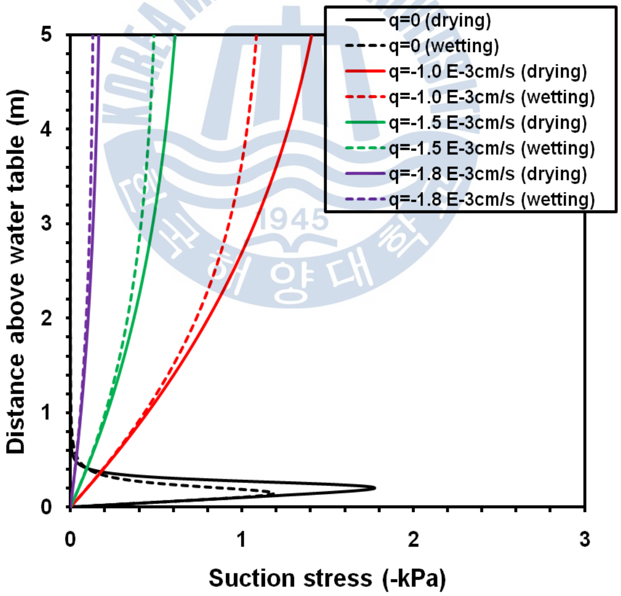

(b) Relationship of distance above water table vs suction stress

Fig. 5.5 Variation for matric suction and suction stress under steady infiltration rates (D_r=60%)

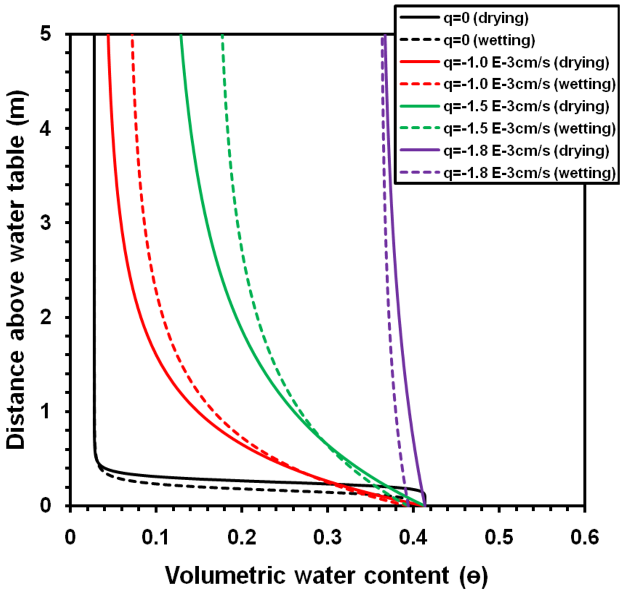

(a) Relationship of distance above water table vs volumetric water content

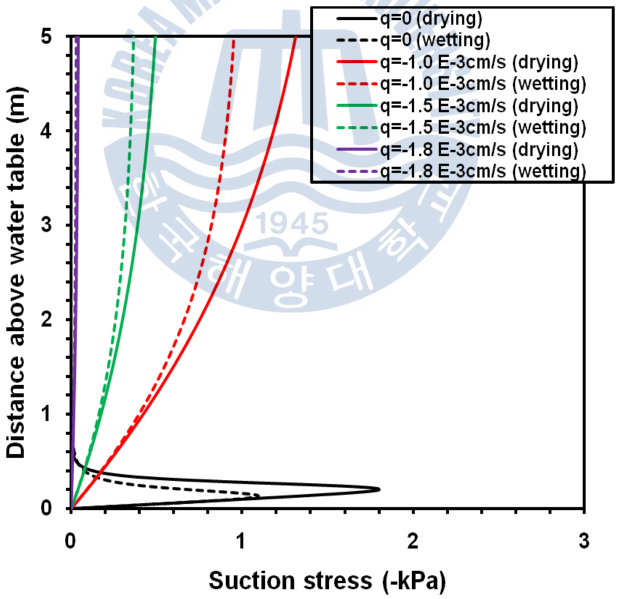

(b) Relationship of distance above water table vs suction stress

Fig. 5.6 Variation for matric suction and suction stress under steady infiltration rates (D_r=75%)

As shown in above figures, the profiles of the volumetric water content are sensitive to the applied infiltration rates, and are varying from nearly zero saturation to nearly full saturation at the ground surface. Variation of volumetric water content is decreased in drying and wetting as infiltration rate is increased. The profiles of suction stress also vary with the variation of infiltration. The value of suction stress is decreased in drying and wetting as infiltration rate is increased. Changing the infiltration rate from 1.5×10^{-3}cm/s to 1.8×10^{-3}cm/s causes a drastic decrease in suction stress into nearly zero but not to zero different with no infiltration. Therefore, increasement of strength is predicted due to suction stress at all depth of slope. Figures 5.7, 5.8, and 5.9 show the relationship between factor of safety and distance above water table for sand slopes. Table 5.2 shows the failure zone of sand slopes under infiltration rate conditions.

Table 5.2 Failure zone of sand slopes under infiltration rate (F_s<1)

Infiltration rate conditions (cm/s)	Failure zone (m) (below the ground surface)		
	D_r=40%	D_r=60%	D_r=75%
0	0~5.0	0~2.5	0~0.2
1.0×10^{-3}	1.5~5.0	-	-
1.5×10^{-3}	0.5~5.0	-	-
1.8×10^{-3}	0.1~5.0	0.2~2.0	-

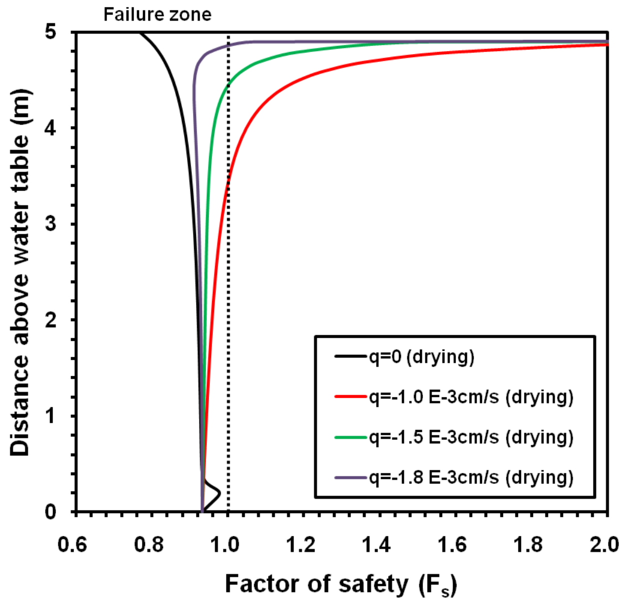

(a) Drying

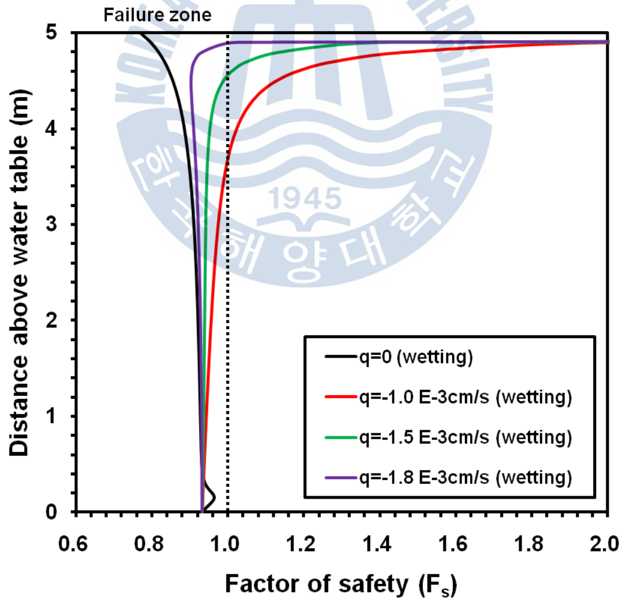

(b) Wetting

Fig. 5.7 Relationship between factor of safety and distance above water table for sand slope (D_r=40%)

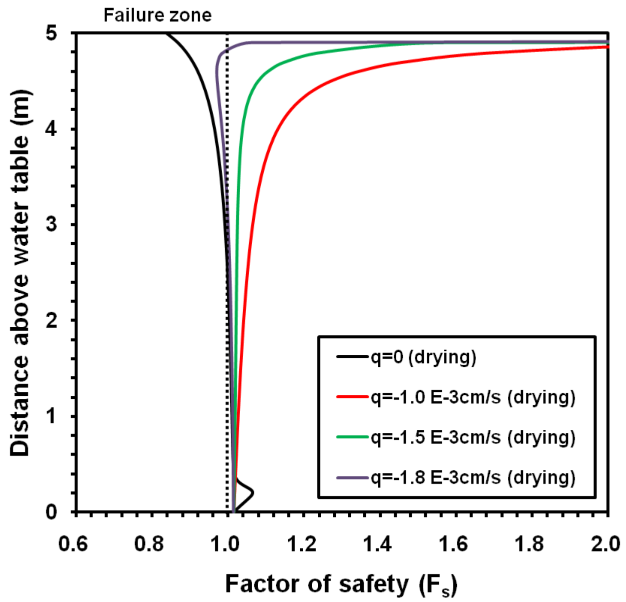

(a) Drying

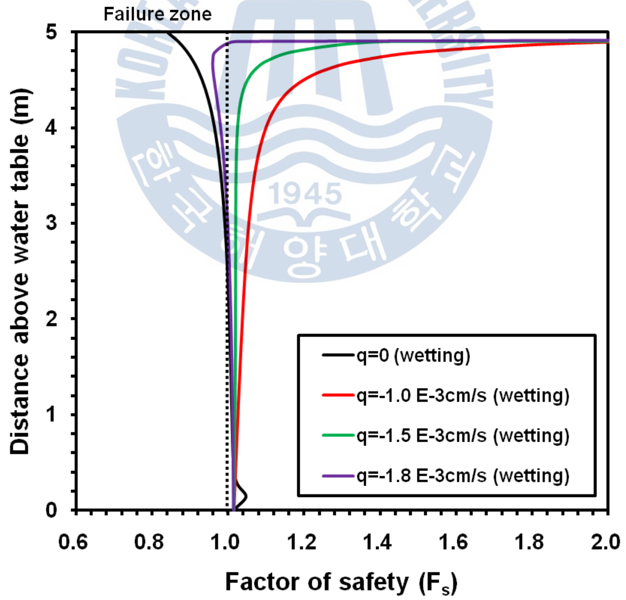

(b) Wetting

Fig. 5.8 Relationship between factor of safety and distance above water table for sand slope (D_r=60%)

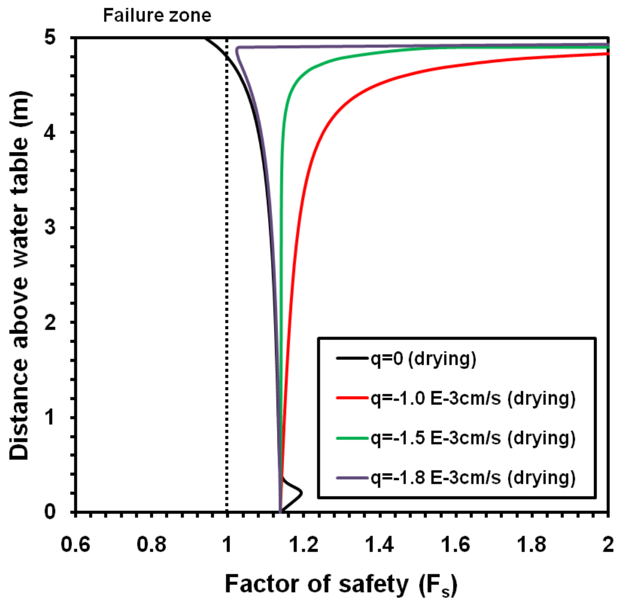

(a) Drying

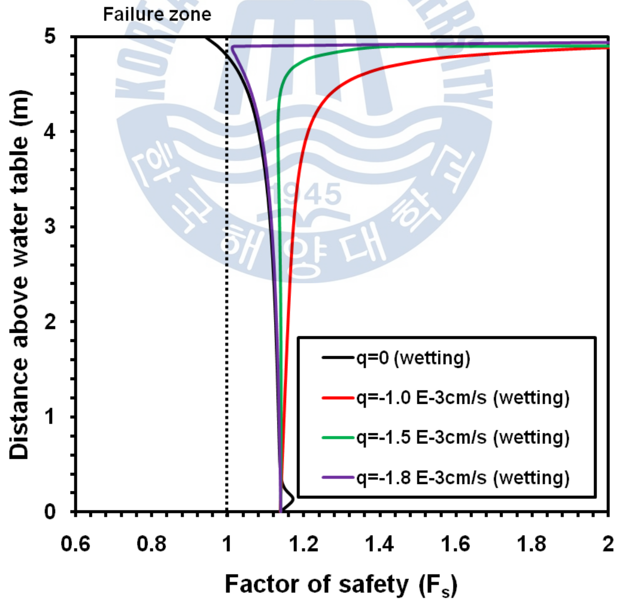

(b) Wetting

Fig. 5.9 Relationship between factor of safety and distance above water table for sand slope (D_r=75%)

Under no infiltration rate condition, factor of safety is increased at the zone between 0 to 0.4m above the water table due to effect for suction stress. However, under infiltration rate condition, factor of safety is increased at the all depth in slope due to effect for suction stress. Of course, as infiltration rate approaches the value of the saturated hydraulic conductivity, stability of sand slope is decreased result from decreasing suction stress. However, slope is maintained in a more stable conditions under infiltration rate condition than no infiltration condition. As indicated in SWCC and SSCC, these results are caused as state of sand is reached to pendular zone at the relatively small matric suction range and suction stress does not occurred in the all slope depth. Therefore, in case of such coarse sand slopes, they show the unstable state by themselves under no infiltration condition.

For the slope composed with relative density of 40% sands, full-scale landslide may be occurred under no infiltration rate and infiltration rates. For the slope composed with relative density of 75% sands, shallow landslide may be occurred enough to be ignored near the ground surface under no infiltration condition. However, for the sand slope composed with relative density of 60%, a zone where the factor of safety is less than 1.0 is observed in the zone between 0m to 2.5m below the ground surface under no infiltration and a zone where the factor of safety is less than 1.0 is observed in a zone between 0.2m to 3.0m below the ground surface under infiltration rate of 1.8×10^{-3}cm/s. Therefore, if rainfall does not occurred or occurred (when q is closed to 1.8×10^{-3}cm/s) on this slope, shallow landslide may be occurred.

Chapter 6. Conclusions

In this study, matric suction and volumetric water content were measured for sand within the range of relative densities 40%, 60%, and 75% according to drying and wetting process using automated Soil Water Characteristic Curve apparatus. As the results, Soil Water Characteristic Curve (SWCC), Hydraulic conductivity function (HCF), and Suction Stress Characteristic Curve (SSCC) were obtained through van Genuchten (1980)'s closed-form equation. Moreover, to assess the stability of unsaturated infinite slope existing water table, slope was assumed that it is composed of sands with the same relative densities 40%, 60%, and 75%, respectively. The results can be summarized as follows.

1. Automated SWCC apparatus can comprehensively assess SWCC of unsaturated soil by conducting the both drying and wetting processes. Moreover, it can minimize errors which can be occurred by experimenter and measure the soil-water characteristic accurately.

2. To understand the characteristic of sand according to relative density, Joomunjin sand was used as experimental sample within the range of relative densities 40%, 60%, and 75%. For drying, as the relative density is increased, Air Entry Value (AEV) and variation of volumetric water content is increased. For wetting process, difference of hysteresis for SWCC is decreased as relative density is increased.

3. The suction stress of sand has increased-and-decreased characteristic as well as maximum suction stress is showed at AEV and suction stress is zero at zero matric suction. Besides, suction stress reaches a maximum value generally less than 0.4m above the water table. For drying process, maximum suction stress is increased as relative density is increased. While, for wetting process, maximum suction stress is decreased as relative density is increased.

4. Analysis of infinite slopes under possible rainfall conditions indicate that variation of friction angle, moisture content, and suction stress all vary greatly above the water table. As the results, for sand slope within the relative densities 40%, 60%, and 75%, as the infiltration rate approaches the value of the saturated hydraulic conductivity, suction stress is closed to zero but not to zero and stability of sand slopes are decreased due to decreasing suction stress.

5. As the stability analysis of unsaturated sand slope, slope are maintained in more stable condition under infiltration rate condition than no infiltration condition. These results are caused as state of sand is reached to pendular zone at the relatively small matric suction range and suction stress does not occurred at all depth in slope. Therefore, in case of these coarse sand slopes, they show the unstable state by themselves under no infiltration conditions. For the slope composed of relative density 60% sand, the zone where the factor of safety is less than 1.0 is observed in a zone between 0.2m to 3.0m below the ground surface under infiltration rate of 1.8×10^{-3}cm/s. Therefore, if rainfall of which infiltration is 1.8×10^{-3}cm/s is occurred on this slope, shallow

landslide may be occurred.

References

1. Abu-Hejleh, A.N., Znicari, D., and Illangasekare, T.H. (1993), "Permeability determination for unsaturated soils", Unsaturated Soils, GSP No.39, ASCE, Houston, S. and Wray, W. CDs., pp.163-174.
2. Alonso, E.E., Gens, A. and Josa, A. (1990) A constitutive model for partially saturated soils, Geotechnique, 40, 405-430.
3. Bishop, A.W. (1959) The principle of effective stress", Teknisk Ukeblad I Samarbeide Med Teknikk, 106(39), 859-863.
4. Brooks, R. H., and Corey, A. T. (1964) Hydraulic properties of porous media, Colorado State University(Fort Collins), Hydrology Paper, 3, March.
5. Campbell, G.S. (1974), "A simple method for determine unsaturated conductivity from moisture retention data", Soil Science, Vol.117, pp.311-314.
6. Campbell, G.S. (1988), "Soil water potential measurement : an overview, Irrigation Science 9 (4), pp.265-273.
7. Chae, J.G., Kim, B.S., Park, S.W. and Kato, S. (2010) Effect of suction on unconfined compressive strength in partly saturated soils, KSCE Journal of Civil Engineering, 14(3), 281-290.
8. Cho, S.E., and Lee, S.R. (2000), "Slope Stability Analysis of Unsaturated Soil Slopes Due to Rainfall Infiltration", Journal of Korean Geotechnical Society, Vol.16, No.1, pp.51-64.
9. Cornforth, D.H. (1973), "Prediction of drained strength of sands from relative density measurement", ASTM STP, No.523, pp.281-303.
10. Cornforth, D.H. (2005), "Landslides in Practice: Investigation, Analysis, and Remedial/preventative Options in Soils", John Wiley and Sons, 596p.
11. Dane, J.H., and Hruska, S. (1983), "In-situ determination of soil hydraulic properties during leaching", Soil Science Society of

America Journal, Vol.47., No.4, pp.619-624.
12. de Campos, T.M.P., Andrade, M.H.N., and Vargas, E.A., Jr. (1991), "Unsaturated colluvium over rock slide in a forested site in Rio de Janeiro, Brazil. Proc. 6th Int. Symp. on landslides, Christchurch New Zealand, Balkema, Rotterdam, The Netherlands, Vol.2, pp.1357-1364.
13. Fredlund, D.G., and Morgenstern, N.R.(1977), "Stress Variables for Unsaturated Soils", Can. Geotech. Eng. Div., ASCE, Vol.103, No. GT5, pp.447-466.
14. Fredlund, D.G., Morgenstern, N.R. and Widger, D.A. (1978) The shear strength of unsaturated soils, Canadian Geotechnical Journal, 15(3), 313-321.
15. Fredlund, D.G. and Rahardjo, H. (1993) Soil mechanics for unsaturated soils, John Wiley & Sons Inc., New York.
16. Fredlund, D. G. and Xing, A. (1994) Equations for the soil-water characteristic curve, Canadian Geotechnical Journal, 31(3), 521-532.
17. Gallipoli, D., Gens, A. Sharma, R. and Vaunat, J. (2003) An elasto-plastic model for unsaturated soil incorporating the effects of suction and degree of saturation on mechanical behavior, Geotechnique, 53, 123-135.
18. Gardner, W.R. (1958), "Steady state solutions of the unsaturated moisture flow equation with application to evaporation from a water table", Soil Sci, Vol.85, pp.228-232.
19. Godt, J.W., Baum, R.L., and Chleborad, A.F. (2006), "Rainfall characteristics for shallow landsliding in Seattle, Washington, USA. Earth Surface Processes and Landforms, Vol.31(1), pp.97-110.
20. Haines, W.B. (1930), "Studies in the physical properties of soil. V. The hysteresis effect in capillary properties and the modes of moisture distribution associated therewith", Jouranl of Agricultural Science, 20, 97-116.
21. Hassler, G.L., and Brunner, E. (1945), "Measurement of capillary pressures in small core samples", Petroleum Technology, Technical Paper, pp.114-123.
22. Hong, W.P., and Kim, Y.W., Kim, S.K., Han, J.G., and Kim M. (1990). "Prediction of Rainfall-triggered Landslides in Korea", Journal of Korean Geotechnical Society, Vol.6, No.2, pp.55-63.

23. Hong, W.P., and Song, Y.S. (2006), "An Experimental Study on the Stabilizing Effect of Nails Against Sliding", Journal of Korean Geotechnical Society, Vol.22, No.2, pp.5-17.
24. Houlsby, G.T. (1997) The work input an unsaturated granular material, Geotechnique, 47, 193-196.
25. Hwang. C.S., and Kim, T.H. (2004), "Determination of the unsaturated Hydraulic Conductivity Function", Journal of Korean Geotechnical Society, Vol.20, No.7, pp.159-169.
26. Israelachvili, J. (1992), "Intermolecular & Surface Forces, 2nd ed., Academic, San Diego.
27. Iwata, S., Tabuchi, T., and Warkentin, B.P. (1995), "Soil-Water Interactions : Mechanisms and Applications, 2nd ed., Marcel Dekker, New York.
28. Jennings, J.E.B. and Burland, J.B. (1962) Limitation to the use of effective stresses in unsaturated soils, Geotechnique, 12, 125-144.
29. Kim, C.K and Kim, T.H. (2010) Behavior of unsaturated weathered residual granite soil with initial water contents, Engineering Geology, 113, 1-10.
30. Kim, K.S., Song, Y.S., Chae, B.G., Cho, Y.C., and Lee. C.O. (2007), "Geometric characteristics of Landslides on Natural Terrain according to the Geological Condition", The Journal of Engineering Geology, Vol.17, No.1, pp.75-87.
31. Kim, S.K., Ryu, C.H. and Song, J.K. (1996), Measurements of Soil-Water Characteristics for Different Unsaturated Soils, Journal of Korean Geotechnical Society, 12(6), 139-151.
32. Kim, T.H. (2001) Moisture-induced tensile strength and cohesion in sand, Ph.D. thesis, Univ. of Colorado at Boulder, CO.
33. Kumar, S., and Malik, R.S. (1990), "Verification of quick capillary rise approach for determining pore geometrical characteristics in soils of varying texture", Soil Science, 150(6), 883-888.
34. Laroussi, C.H., and Debacker, L.W. (1979), "Relations between geometrical properties of glass bead media and their main $\Psi(\theta)$ hysteresis loops", Soil Science Society of America Journal, 43, 646-650.

35. Letey, J., Osborn, J., and Pelishek, R.E. (1962), "Measurement of liquid-solid contact angles in soil and sand", Soil Science, 93, 149-153.
36. Lu, N., and Likos, W.J. (2004) Unsaturated soil mechanics, John Wiley & Sons Inc., New York.
37. Lu, N., and Godt. J.(2008), "Infinite-Slope Stability under Steady Unsaturated Seepage Conditions", Water Resources Research, Vol.44, W11404, pp.1-13.
38. Lu, N., Godt, J.W. and D.T. Wu (2010) A closed-form equation for effective stress in unsaturated soil, Water Resources Research, 46, W05515.
39. Lu, N., and Griffiths, D.V., (2004), "Suction stress profiles in unsaturated soils, Journal of Geotechnical and Geoenvironmental Engineering, Vol.130(10), pp.1063-1076.
40. Lu, N., Kim, T.-H. Sture, S. and Likos, W.J. (2009) Tensile strength of unsaturated sand, Journal of Engineering Mechanics, 135(12), 1410-1419.
41. Lu, N. and Likos, W.J. (2006) Suction stress characteristic curve for unsaturated soil, Journal of Geotechnical and Geoenvironmental Engineering, 132(2), 131-142.
42. Lu, N., Wu, B., and Tan, C.P. (2007), "Tensile strength characteristics of unsaturated sands", Journal of Geotechnical and Geoenviromental Engineering, ASCE, Vol.133, No.2, pp.144-154.
43. Marachi, N.D., Chan, C.K., Seed, H.B., and Duncan, J.M. (1969), Strength and Deformation Characteristics of Rockfill Materials, University of california Report TE-69-5, Berkeley, California.
44. Matyas, E.L. and Radhakrishna, H.S. (1968) Volume change characteristics of partially saturated soils, Geotechnique, 18, 432-448.
45. Mualem, Y. (1976), "A new model for predicting the hydraulic conductivity of unsaturated porous media", Water Resources Research, 12(3), 513-522.
46. Mualem, Y. (1984), "A modified dependent domain theory of hyteresis", Soil Science, 137, 283-291.
47. Nam, S., Gutierrez, M., Diplas, P., Petrie. J., Wayllace, A., Lu. N.,

and Munoz, J.J. (2009), "Comparison of testing techniques and models for establishing the SWCC of riverbank soils", Engineering Geology, 110, pp.1-10.

48. Nimmo, J., Akstin, K., and Mello, K. (1992), "Improved apparatus for measuring hydraulic conductivity at low water content", Soil Science Society of America Journal, 56, 1758-1761.
49. Or, D., Wraith, J.M. (1999), "Soil water content and water potential relationships. In: Sumner, M.E. (Ed.), Handbook of Soil science. CRC Press, Boca Raton, FL, pp. A53-A85.
50. Park, D.K., Oh, J.R., Son, Y.J., Park, J.H., and Lee, M.S. (2008), "Steep slope management system in Korea", Proc. the 2nd East Asia Landslides Symposium, Seoul, pp.7-11.
51. Richards, L.A. (1931), "Capillary conduction of liquids in porous media", Journal of Applied physics, Vol.1, pp.318-333.
52. Rowe, P.W., (1969), "The relation between the shear strenth of sands in triaxial compression, plane strain and direct shear", Geotechnique, Vol.19(1), pp.75-80.
53. Schubert, H. (1975) Tensile strength of agglomerates, Powder Technology, 11, 107-119.
54. Song, Y.S., Lee, N.W., Hwang, W.K., and Kim. T.H. (2010), "Construction and Application of an Automated Apparatus for Calculating the Soil-Water Characteristic Curve", Korean Society of Engineering Geology, Vol.20, No.3, pp.281-295.
55. Terzaghi, K. (1943) Theoretical soil mechanics, John Wiley & Sons Inc., New York.
56. density Genuchten, M.T. (1980) A closed-form equation for predicting the hydraulic conductivity of unsaturated soils, Soil Science Society of America Journal, 44, 892-898.
57. Welge. H.J. (1952), "A simplified method for computing oil recovery by gas or water drive", Transactions AIME, Vol.195, pp.91-98.
58. Wildenschild, D., Jensen, K.H., Hollenbeck, K.J., Illangasekare, T.H.,Znicari, D., Sonnenborg, T., and Butts, M.B. (1997), " A two-stage procedure for determining unsaturated hydraulic characteristics using a syringe pump and outflow observations", Soil Science Society of America Journal, Vol.61, pp.347-359.

59. Wolle, C.M., and Hachich, W. (1989), "Rain-induced landslides in southeastern Brazil", Proceedings of the 12th International Conference on Soil Mechanics and Foundation Engineering, Roi de Janeiro, pp.1639-1644.
60. Zachman, D.W., Duchateau, P.C., and Klute, A., (1981), "The calibration of the Richards flow equation for a draining column by parameter identification", Soil Science Society of America Journal, Vol.45, pp.1012-1015.

Acknowledgements

이 논문이 완성되기까지 많은 도움을 주신 여러분들께 진심으로 감사를 드립니다. 먼저 학부에서부터 석사까지 학업을 수행 할 수 있도록 많은 가르침을 주시고 부족한 저를 아낌없이 이끌어 주신 김태형 지도교수님과 많이 부족하고 무딘 저를 다듬어 주시고 훈련시켜 석사학위논문이 나오도록 도와주신 송영석 박사님께 깊은 감사의 말씀을 전합니다. 또한 부족한 논문을 심사해주시고 가르침을 주신 서영교 교수님께도 감사드립니다.

토목공학이라는 멋진 학문을 가르쳐주시고 장난기 많은 저를 너그럽게 이해해주신 김태곤 교수님, 이중우 교수님, 김도삼 교수님, 경갑수 교수님께 감사드립니다. 또한 한국지질자원연구원에서 많은 격려와 가르침, 조언을 아끼지 않으셨던 김원영 박사님, 이병주 박사님, 이춘오 박사님, 김경수 박사님, 김재곤 박사님, 채병곤 실장님, 조용찬 박사님, 정승원 박사님, 남인현 박사님, 최정해 박사님께도 감사의 마음을 전합니다.

논문을 쓰는 동안 많은 충고와 격려를 해준 지반공학연구실에 수정이 누나, 학부 및 대학원 생활동안 멘토가 되어준 존경하는 웅기형 감사했습니다. 그리고 내 동기이자 형제인 영준이, 늘 고생하는 잠 많은 성규, 곧 미국으로 유학갈 성준이, 이번에 들어온 귀여운 민아도 항상 고맙다. 그 밖에 지반공학 연구실에 길잡이가 되어주신 기천이형, 정현이형, 용수형, 중호형, 외부에 있는 저를 행정적으로 뒷받침해준 김지향 조교누나께도 감사의 말씀을 전하고 싶습니다. 또한 연구원에서 2년 동안 함께 공부하고 인생의 고민을 나누었던 진웅이형, 그 밖에 춘오형, 동완, 규보, 세은, 영우, 지원, 숙현이도 고맙고 연구원 생활 잘 하길 기원하겠습니다.

2011년에는 우리 02학번 동기들 (선욱, 현기, 영준, 상길, 성진) 모두 준비 잘해서 취업 잘 되길 기원하고 재학아, 길태야, 선현아 회사생활 열심히 해. 그리고 토목과 최고 미녀 민지와 (박)소연이도 무궁한 발전이 있길 바란다. 무엇

보다 언제나 저의 편에 서서 용기와 사랑을 주신 가족들에게도 감사의 마음을 전합니다.

마지막으로 언제나 나를 웃게 해주고 내게 힘이 되어준 선영아~ 고마워.^^ 이상으로 항상 발전하고 누구에게나 귀감이 되는 이남우가 될 것을 다짐하며 이 논문을 마칩니다. 감사합니다.